Advanced Multi-material Electronic and Optoelectronic Fibers and Textiles

*Wei Yan, Alexis Page, Tung Nguyen, Yunpeng Qu, Federica Sordo, Lei Wei and Fabien Sorin**

W. Yan, A. G. Page, Dr. D. T. Nguyên, Dr. Y. Qu, Prof. F. Sorin
Laboratory of Photonic Materials and Fibre Devices (FIMAP), Institute of Materials, Ecole Polytechnique Fédérale de Lausanne (EPFL)
Lausanne 1015, Switzerland
* E-mail: fabien.sorin@epfl.ch

Prof. L. Wei
School of Electrical and Electronic Engineering
Nanyang Technological University, Singapore

Keywords: (multi-material fibers, hybrid optical fibers, thermal drawing, functional textiles)

Abstract

The ability to integrate complex electronic and optoelectronic functionalities within soft and thin fibers is one of today's key advanced manufacturing challenges. Multi-functional and connected fiber devices will be at the heart of the development of smart textiles and wearable devices. They also offer novel opportunities for surgical probes and tools, robotics and prostheses, communication systems, and portable energy harvesters. Among the various fiber processing methods, the preform-to-fiber thermal drawing technique is a promising tool to fabricate fibers with complex multi-material architectures at the micro- and nanoscales. In this progress report, we review the milestones that have led to the advanced multi-material fibers integrating metals, semiconductors, and functional polymers with various device architectures and functionalities. We then present recent breakthroughs in the fundamental understanding of the fluid dynamics and rheology, as well as the tailoring of material microstructures at play in the thermal drawing process. Finally, we discuss how this will shape scientific research and how it offers significant new opportunities for this rapidly growing and active scientific and technological field.

Introduction

Advanced functionalities are a result of the combination of different materials, at the right scales and organized within the proper architecture. Decades of research have been devoted to the fabrication of nanoscale multi-material structures onto planar and rigid substrates, with the success of silicon wafer-based technologies as a case in point. [1][2] A new materials science and processing challenge has arisen in recent years as an increasing number of application fields have required the integration of nanoscale devices and advanced functionalities onto soft and non-planar substrates. Several strategies have been proposed in order to realize electronic and optoelectronic devices that could reconcile high performance and mechanical

deformation.[3][4] Within the field of flexible electronics, fiber-based devices are rapidly developing as an alternative platform that can offer functionality in a variety of configurations in which elongated aspect ratios or textile–like properties are required.[5][6][7][8][9] In particular, the progress of fiber processing technologies reveals the ubiquitous nature of fibers via their exploitation in novel fields of applications. Advanced fibers are envisioned to be the next generation of optical probes for sensing[10] and minimally invasive surgical tools.[11] They can also serve as scaffolds, form bioengineered tissues, act as active releasing components in sutures or wound healing bandages, and form sensing fabrics for personalize care and physiological parameters monitoring, or in soft prostheses.[12] Electronic and optical fibers can also form a variety of two- and three-dimensional sensing networks such as those integrated in robotics or within structures and composites for health monitoring. [13] Moreover, they can also be ideal for large area flexible energy harvesting and storage systems, using either mechanical or light energy sources. [14][15] More importantly, they will constitute the next generation of smart textiles for which added functionalities will come not from embedded point devices but from the individual textile fibers themselves.[16]

To realize the promise of advanced fiber-based devices, novel functionalities must be integrated beyond optical transport, thermal insulation, or passive mechanical attributes. Electronic and optoelectronic functionalities are of particular interest but require the integration of materials with drastically different electronic properties, organized at the sub-micrometer scale, and within prescribed architectures. However, the functionalization of the peculiar fiber geometry, aspect ratio, and materials remains challenging. The first approach consists in adapting conventional deposition techniques to coat a variety of mostly spun fiber-shaped substrates or fabrics with functional materials. Since then, tremendous advances in such fabrication methods have been developed over the past decades. They include, but are not limited to, hydrothermally chemical growth,[17] electrodeposition,[18] electrochemical anodization,[19] synthesis via electroless plating,[20] physical convolution or wrapping,[21] physical vapor deposition,[22] chemical vapor deposition,[23] electrochemical deposition,[24] spin-coating,[25] dip coating,[26] anodizing,[24] electrospinning,[27] printing,[28], pad-dry-cure in textile industry.[29] These approaches hold great promise for textile-integrated energy harvesting and storage, as well as for applications in personal care, sport and fashion. We will not review this field in this report, but instead refer the reader to a variety of relevant publications, including exhaustive reviews. [30][31][32][33][34][35][36][37]

The field of Multi-material fibers

The core technique that will be at the heart of this report consists in exploiting another fiber processing method called thermal drawing, originally used to make optical fibers. [5] While developed for a large part by optical engineers, this process has triggered an increasing interest from the materials science and engineering community due to its unique control that allows over the complex architectures and feature sizes of the fibers created using this method. It was also shown that it could be applied to a wide range of polymers and glasses, as well as conducting and semiconducting materials. This has inspired materials scientists to embrace thermal drawing as a fabrication approach to make fibers with advanced functionalities

beyond optical transport, creating the field of “multi-material fibers” or ‘hybrid optical fibers”. Compared to the fabrication approach described above that consists in the coating of spun fibers, multi-material fibers use thermal drawing mainly in two ways: the first one is via the drawing of a micro-structured polymer or glass fiber that act as a substrate for the integration of functional materials at prescribed positions. The second one is to directly co-draw all of the materials together previously assembled in a macroscopic preform with larger feature sizes and within prescribed architecture.

Multi-material thermal drawing has the unique advantage of enabling complex and multiple functionalities within fibers that can be of arbitrary shape and integrate a variety of textures. It is also amenable to the integration of complex electronic and optoelectronic functionalities via the processing of inorganic semiconducting materials with nanometer feature sizes. As we will discuss in this report, some integrated fiber devices have reached the performance comparable with traditional, two-dimensional electronic and optoelectronic devices. While the idea of integrating materials other than conventional glass or polymers was first exploited to create fibers with novel optical properties, it was the development of electronic and optoelectronic structures that truly positioned the field of multi-material fibers as a way to impart optical fibers with other functionalities. In the last fifteen years, this method has been used to fabricate a variety of fibers that integrate glasses, polymers, polymer composites, metals, semiconductors, and dielectrics.[38][39][40][41][42] These materials could be integrated into the forms of fiber cores, micro- and nanowires or thin-films, and positioned at any place in the fiber cross-section. The first generation of such multi-material fibers has opened a great breadth of novel opportunities for applications in sensing, energy harvesting, optical probes and surgery tools, robotics, and smart textiles. [5][43][44]

Objectives of this progress report

After the first industrial application of multi-material fibers as minimally invasive surgical tools by the company Omniguide inc, research in the field has consisted for a large part in exploiting Until recently, however, one application for multi-material fibers has reached the market, via the company OmniGuide, which makes hollow core photonic bandgap fibers for minimally-invasive surgery. The integration of electronic and optoelectronic functionalities has been an influential innovation in materials science and processing, but the performance of the in-fiber devices and the type of applications and functionalities made possible have remained limited. For a field to keep its momentum, it is essential to have more developments towards the next generation of fiber devices beyond proof-of-concept. This requires addressing engineering bottlenecks, finding novel applications, and most importantly to continue deepening the fundamental understanding of the materials and processes at play to further improve device performance and functionalities. In the past few years, a series of scientific and technological breakthroughs are starting to alleviate these challenges, and are presenting exciting new opportunities for this rapidly growing field. Deeper understanding of the materials science aspects behind the viscous flow of materials during and after drawing, and of the materials composition and their microstructure, has led to the ability to integrate more functionalities within devices exhibiting better performance. At the same time, the development of

engineering solutions and novel applications has enriched the multi-material fiber platform, maintaining a growing interest within both academia and industry.

The objective of this progress report is not to provide an exhaustive review on the field of multi-material fibers, but rather to describe in detail the recent scientific and technological breakthroughs that are reshaping this field. For the purpose of this manuscript, we define a “multi-material fiber” as any fiber for which the main cladding is made via thermal drawing. We focus particularly on fibers with electronic and optoelectronic functionalities, as recent advances have primarily been made for these fibers. Thermal drawing allows for the integration of a variety of materials in different shapes, including inorganic semiconductors commonly used in optoelectronic in nanowire form. The different materials used are a rich topic for scientific research and innovation, and the integration of such advanced functionalities starts to bring novel applications for both functional polymer and glass fibers.

Detailed content of this report

In Section 1, we will remind the reader of the materials and processes that are used to make multi-material fibers. Then in Section 2, we will briefly review the different types of fiber architectures and functionalities achieved thus far, focusing primarily on electronic and optoelectronic developments. In Sections three to five, we will present recent scientific and technological breakthroughs that are profoundly impacting the field of multi-material fibers. This discussion is divided into three sections, representing the three pillars onto which functionalities are built: (1) combining materials with different properties: we will present the new materials that have been recently found to be compatible with the thermal drawing process, how they were discovered, and the implications for applications; (2) organizing the materials in the proper nanoscale architectures: we will show how a deeper understanding of the viscous flow process and rheological properties allows for finer and more complex architectures; (3) controlling the microstructure: focusing particularly on semiconducting materials, we will show how novel crystallization schemes can elegantly control crystal nucleation and growth and, ultimately, the grain size, element segregation, and crystallographic orientation of electronic and optoelectronic fibers. In the last section, we will discuss the novel applications being made possible by these materials science and processing breakthroughs. We will also discuss how combining these advances into a single fiber opens new opportunities in a variety of fields. Finally, as functionality is also a matter of device density, we will discuss how multiple devices can be integrated in a single fiber, and how fiber assemblies such as textiles are becoming a major type of application for multi-material fibers.

1. Processes, basic materials requirements, and fabrication methods

1.1 Direct multi-material drawing

The majority of optical fibers used in communication systems are fabricated from a main material–silica glass. Pulling a macroscopic preform made out of a silica cladding and a doped silica core, above the softening temperature of silica produces hundreds-of-kilometers long, highly uniform and low-loss optical fibers. Exploiting the same principle, a new family of multi-material fibers integrating different materials with disparate properties has arisen. [5][43][45][46] This approach typically starts with preparing a multi-material macroscopic preform in which bulk materials are arranged at prescribed positions with a well-defined geometry, as shown schematically in Figure 1a. Many different methods can be used to make preforms, such as thin-film rolling, [38][47] consolidation of materials in a vacuum oven or in a hot press, the stack-and-draw approach, [48][49] extrusion, [50][51] the rod-in-tube approach, [52] the double-crucible approach, [53][54] and additive manufacturing. [55] The resulting preform is then fed into a furnace where all the constituting materials soften or melt. An external force applied by a capstan pulls the preform into a fiber (Figure 1b), the size of which can be tuned by controlling the drawing temperature, the feeding speed of the preform, and the drawing speed. While it can be engineered otherwise, the resulting long fiber usually has the same composition and geometry of the initial preform, but with a geometric scale down of all dimensions in its cross-section. The multi-material thermal drawing approach exhibits several intriguing characteristics. First of all, as the preform is structured at the millimeter scale, a complex cross-section with controllable positioning of multiple materials can be easily obtained. Fibers that maintain the cross sectional architecture of the preform during drawing can therefore be endowed with sophisticated architectures. Simultaneously, multiple device configurations can be designed into the preform, leading to a single fiber with a high density of devices and multiple functionalities. Next, nanoscale feature sizes can be achieved, which results in electronic and optoelectronic fibers whose performance can be on par with their planar counterparts. Fiber devices are also versatile and can be used alone or integrated within a variety of configurations including meshes, screens, fabrics, and textiles. Finally, from a processing point of view, by the law of mass conservation, scaling down a macroscopic preform results in potentially kilometers-long thin fibers in a short time. They require minimal post processing as they are drawn with a cladding that can protect the encapsulated functional materials and make the fiber robust against washing or other difficult

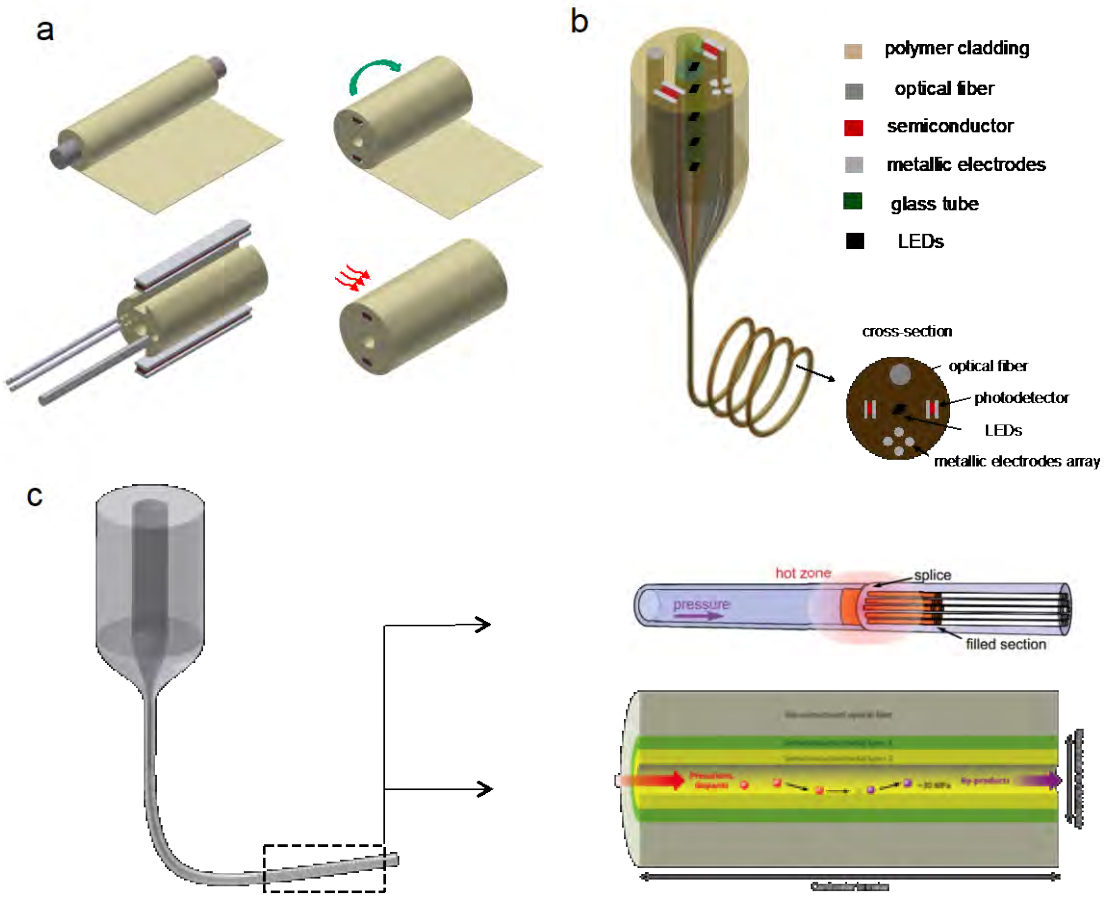

Figure 1. Fabrication of multi-material fibers. a) Schematic of preform making. b) Thermal drawing of multi-material fibers. c) Microstructured optical fibers are functionalized via pressure-assisted melt filling and HPCVD techniques. Reproduced with permissions.[1][2] Copyright 2011, OSA and copyright 2013, Annual Reviews

conditions. The cladding material can also be tailored to be optically transparent, mechanically soft, or even biodegradable, as we will see in the following sections.

In order to maintain the identical architecture and cross-sectional integrity of the preform along the fiber length, we briefly describe some criteria for the co-drawing of different materials with disparate thermomechanical properties (a more complete discussion can be found in references[5][44]). First, the cladding, which encapsulates all other materials and supports most of the stress, must be processed at a relatively high viscosity, typically between 10^4 and 10^8 Pa·s. Amorphous materials that exhibit a continuous change of viscosity with respect to temperature such as glasses and thermoplastics are therefore good candidates. A more precise rheological criterion has been recently proposed, [56] which we describe in Section 3. Second, the processing temperature window (between the glass transition and crystallization temperatures) should be large enough that the amorphous material does not crystallize before it is plastically deformed. When different polymers or glasses are combined into a single fiber, they should exhibit compatible viscosities at the drawing temperature, so they can be co-drawn, and to avoid deformation and delamination at the interface. Next, when crystalline materials are incorporated, their melting point should

be lower than the drawing temperature so that they can flow in the fiber as a melt. Materials that interface with crystalline materials should not be in the liquid state during drawing, to avoid mixing. Also, potential chemical diffusion and reaction must be anticipated and can be exploited to form novel materials inside functional fibers as discussed in Section 3. Finally, all amorphous materials must have relatively similar thermal expansion coefficients at the drawing temperature to avoid the formation of cracks and fractures and limit the residual stress in fibers.

1.2 Post-thermal drawing fabrications

Besides the direct thermal drawing of fibers from multi-material preforms, thermal drawing can also be used to fabricate microstructured optical fibers (MOFs) as a substrate onto or within which materials can be deposited. The first technique consists in the filling of materials in the molten state pressured inside the prescribed structure of micrometer scale capillaries inside the fiber, as shown schematically in Figure 1c. It was experimentally shown that the pressure-assisted melt filling approach allows the filling of a variety of functional materials into the fiber platform, such as metallic nanowires, [57] dielectric materials, [58] semiconductors[59] and chalcogenide glasses[60]. A more exhaustive description about the characteristics and applications of this approach can be found in a recent review. [44] A second approach to fill the MOFs relies on high-pressure chemical vapor deposition (HPCVD). A very high pressure (10 to 100 MPa) flow of materials in the gas phase ensures a perfect conformal deposition onto the walls of the long and narrow capillaries of MOFs, eliminating mass-transport constraints and enabling highly uniform coating. It was demonstrated that metals, single-crystal semiconductors, and polycrystalline elemental or compound semiconductor wires with diameters of microscale down to the nanoscale could be fabricated. [61] By controlling the processing temperature and the size of the pores in the fiber, the morphology, crystallinity and crystallographic orientation of functional materials can also be tailored. [61] A key advantage of this approach is the ability to sequentially change the gas composition during deposition, which allows for the fabrication of coaxial homo- and hetero-junctions. A more exhaustive review of this technique can be found in reference. [62]

Other approaches exist to functionalize locally MOFs, most prominently the tip of the fibers or a local region of the fiber cladding, that are commonly regrouped in the “Lab-on-Fiber” technology field. Several approaches have been developed, such as: 1) the direct patterning of the flat tip of optical fibers via nanofabrication techniques. Both top-down, namely photolithography, interference lithography, electron-beam lithography, laser writing, nanoimprinting, focused ion beam milling, etc., and bottom-up methods, e.g., self-assembly, have been successfully demonstrated. Examples of nanostructures on optical fiber tips, their fabrication techniques, and their applications have been reviewed in detail by Kostovski et al. [63][64] 2) Pattern transferring method. Metallic or dielectric structures are first fabricated onto planar substrates using standard nanofabrication techniques or the “nanoskiving” technique before they are transferred onto optical fiber facets. [65][66][67] 3) Direct coating or deposition method. Nanostructured functional materials like carbon nanotube, 2D materials, metallic or dielectric thin films and nanoparticle are coated or deposited at

the tip, outer surface or the internal channel of fibers. [68] Such fibers with functionalized cladding have been mainly proposed for chemical and biological analysis via the optical spectroscopy analysis of the transmitted light. [69] Apart from using similar approaches to contact metallic electrodes embedded within fibers, such approaches have not been used to integrate purely electronic or optoelectronic functionalities.

2. Achieved fiber architectures and functionalities

The different fabrication approaches described above have led to a variety of reported fiber architectures and functionalities. Focusing on electronic and optoelectronic functionalities, we briefly review below such fibers that result either from a direct multi-material drawing approach, or from post-drawing treatments.

2.1 Electronic fibers

Electronic functionalities can be separated into three main categories depending on the conductivity value of the electronic material: metals and polymer composites with high electric conductivity are used as electrodes or resistors; semi-conducting materials are exploited for the ability to modulate their current density mostly via a filed effect; and insulating materials are used for their dielectric (capacitive, piezo- or ferroelectric, etc…) functionalities. Since the first integration of metals within silica fibers using the Taylor process, all of these functionalities have been exploited in electronic fiber devices. The simplest use of metals and conducting polymer composites is as electrodes interfacing with materials outside of the fiber construct. The most explored application for optical fibers integrating an array of such electrodes is neural probes in bioengineering. Thermal drawing constitutes indeed a unique approach to efficiently integrate within flexible fibers a variety of stimulations route for neurons and nerves such as optical, electrical or even chemical. Several demonstrations of fibers integrating a

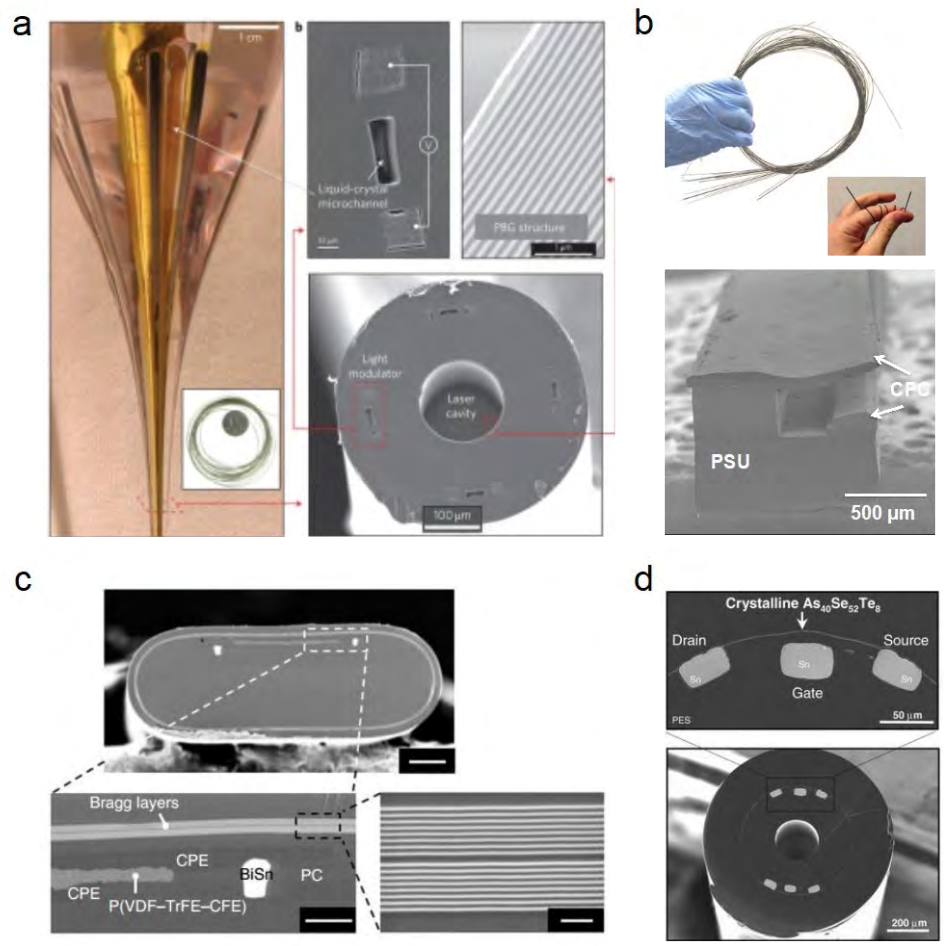

Figure 2. a) An azimuthally polarized radial fiber laser. Reproduced with permissions.[3] Copyright 2012, Springer Nature. b) Electro-mechanical fiber sensors. Reproduced with permissions.[4] Copyright 2017, IOP Publishing. c) Electrostrictive microelectromechanical fibers. Reproduced with permissions.[5] Copyright 2017, Springer Nature. d) A fiber field-effect device. Reproduced with permissions.[6] Copyright 2010, WILEY-VCH Verlag GmbH & Co. KGaA, Wein-heim

step index waveguide surrounded by metallic or composite polymer electrodes have been fabricated and exploited for neural interface. [70] In the discussion in Section 6, we will discuss these structures in greater detail as a case in point for the development of advanced fibers based on novel fundamental understating of the materials and processes at play.

Metallic electrodes can also be used to impose a potential drop across a given domain inside a fiber, to modulate a signal, as shown in Figure 2a. Based on this principle, an azimuthally polarized radial fiber laser was demonstrated that integrated an array of electrically contacted liquid-crystal microchannels encircling the laser cavity in the fiber core.[71] The applied electric field modulated the polarized wavefront emanating from the core, leading to a laser with a dynamically controlled intensity distribution passing through the full azimuthal angular rang. [72][73] Optical fibers with modulated polarization could also be created thanks to large electrodes running along the fiber core and heated via the joule effect. [74] A last example of exploiting electrical conductivity involves polymer composites that are not as efficient conductors as crystalline metals, but can serve as resistors to control the drop of potential along the fiber axis. This has been exploited to

localize a point of illumination along a photodetecting fiber[75], as we will explain in the next section. It has also been used to localize pressure along an electro-mechanical fiber sensor, that integrate a switch-like structure where a bendable thin polymer composite film is drawn on top of an other polymer composite electrode, as shown in Figure 2b[76]. When pressure is applied, a circuit is closed and a current can go from one electrode to the other. This current will depend upon the path along the electrode up to the point of contact, and hence is a function of the applied pressure position.

Thermally drawn electronic fibers could also exploit the dielectric properties of some polymers. For example, all-in-fiber capacitors with a capacitive response up to 20kHz were created, among other configurations, [77][78] by integrating carbon-black loaded polyethylene (CPE) electrodes separated by a poly(vinylidene fluoride) (PVDF) dielectric layer. [79] Using a poly(vinylidene-fluoride-trifluoroethylene) copolymer (P(VDF-TrFE) that crystallizes directly into a piezoelectric phase after thermal drawing, a piezoelectric fiber was created that was able to both emit and detect acoustic radiation over a broad acoustic frequency range, from the tens of Hz to the tens of MHz. [40] The structure of such fiber is shown in Figure 2c. Optimizing the design of the fiber architecture by folding multiple piezoelectric layers was shown to enhance the transducer performance, while assembling multiple fibers into arrays enabled coherent interferences and beam steering. [80] These large-area acoustic fiber devices paved the way toward novel applications in distributed pressure sensing, acoustic sensing and positioning, flow measurement, energy conversion, and communication transceivers.[81]

Finally, semiconductor-based electronic fibers have also been demonstrated. A fiber field-effect transistor that consists of a metallic source/drain and gate as well as a chalcogenide semiconducting thin film has been reported, holding promise for the fabrication of fiber-based discrete logic elements capable of digital signal processing, [82] as shown in Figure 2d. The ability to integrate thermal sensitive semiconductors whose electrical conductivity varies with small changes in temperature into fibers has allowed for large-contact-area heat sensing at a high spatial resolution. [83] When such thermally-sensitive elements were assembled in the vicinity of a hollow-core photonic bandgap fiber core, the electrical single change was able to distinguish normal transmission conditions from those with a leakage caused by heat-generated defects on the fiber. [42] Another intriguing example is an ovonic memory-switching fiber where the built-in electric field modulates the electronic structure of the semiconductor, creating a high-resistance amorphous state and a low-resistance crystalline state. [84] It was shown that the fiber was capable of switching between the ON and OFF states under current pulses of variable intensity.

2.2 Optoelectronic fibers

Having metallic electrodes interfacing with semiconducting domains also opens the possibility for optoelectronic functionalities. The first types of demonstrated optoelectronic fibers integrated metals and polymer composites in contact with chalcogenide semiconductors within a transparent thermoplastic cladding. Chalcogenide glasses are formed based on the chalcogen elements S, Se, and Te or by the addition of other elements such as As, Ge, Sn, or Ga. [85] These glasses exhibit unique optical properties, such as a

wide range of transparency in the infrared, a large refractive index, high optical nonlinearity, and phase change attributes. Their functional and processing attributes can be widely tailored by changing their composition, which makes this class of materials highly versatile. In particular, some compositions such as pure Selenium that was one of the first element investigated for its optoelectronic properties,[86] are very sensitive to irradiation in the visible range, making them excellent for photodetecting applications.

The first metal-semiconductor-insulator optoelectronic fiber fabricated by thermal drawing was demonstrated in 2004. [39] The fiber comprised an amorphous chalcogenide glass core ($As_{40}Se_{50}Te_{10}Sn_5$) contacted by four metallic microwires and encapsulated by a transparent polymer cladding, as shown in Figure 3a. Light incoming on the external surface of the fiber along its length could be detected via a simple photoconducting mechanism. Weaving these fibers into well positioned optical arrays allowed a follow-up study to extract both the amplitude and phase of an electromagnetic field over large areas for lens-less imaging systems. [41] Going from a semiconducting core configuration to a thin-film geometry allowed drastically reduction of the dark current and hence enhanced sensitivity. Cascaded thin films could then be fabricated within a single fiber that integrated several photodetecting devices with feature sizes down to 100 nm. This fiber was able to discriminate wavelengths in the visible range at less than 5 nm resolution and measure the angle of incidence down to a 4° angular resolution. [87] Such complex cross-sectional architecture shown in Figure 3b is a case in point of the complex hybrid nano-scale architectures that can be fabricated in the fiber form thanks to multi-material thermal drawing. Moreover, assembling these fibers into two-dimensional grids led to fabrics that could localize an illumination point, but also perform complex optical tasks such as the lens-less imaging of an object. [41][87] Another potential application of such photosensitive fibers lies in the remote and distributed chemical sensing. [88] In one study, a chalcogenide glass ($Se_{97}S_3$) layer was surrounding a hollow core coated with a specific polymer layer. Upon exposure to a targeted analyte, in this case TATP explosives, a chemiluminescent signal could be detected with a resolution of below 10 ppb. Note that Se, Te, and their compounds composing the fiber

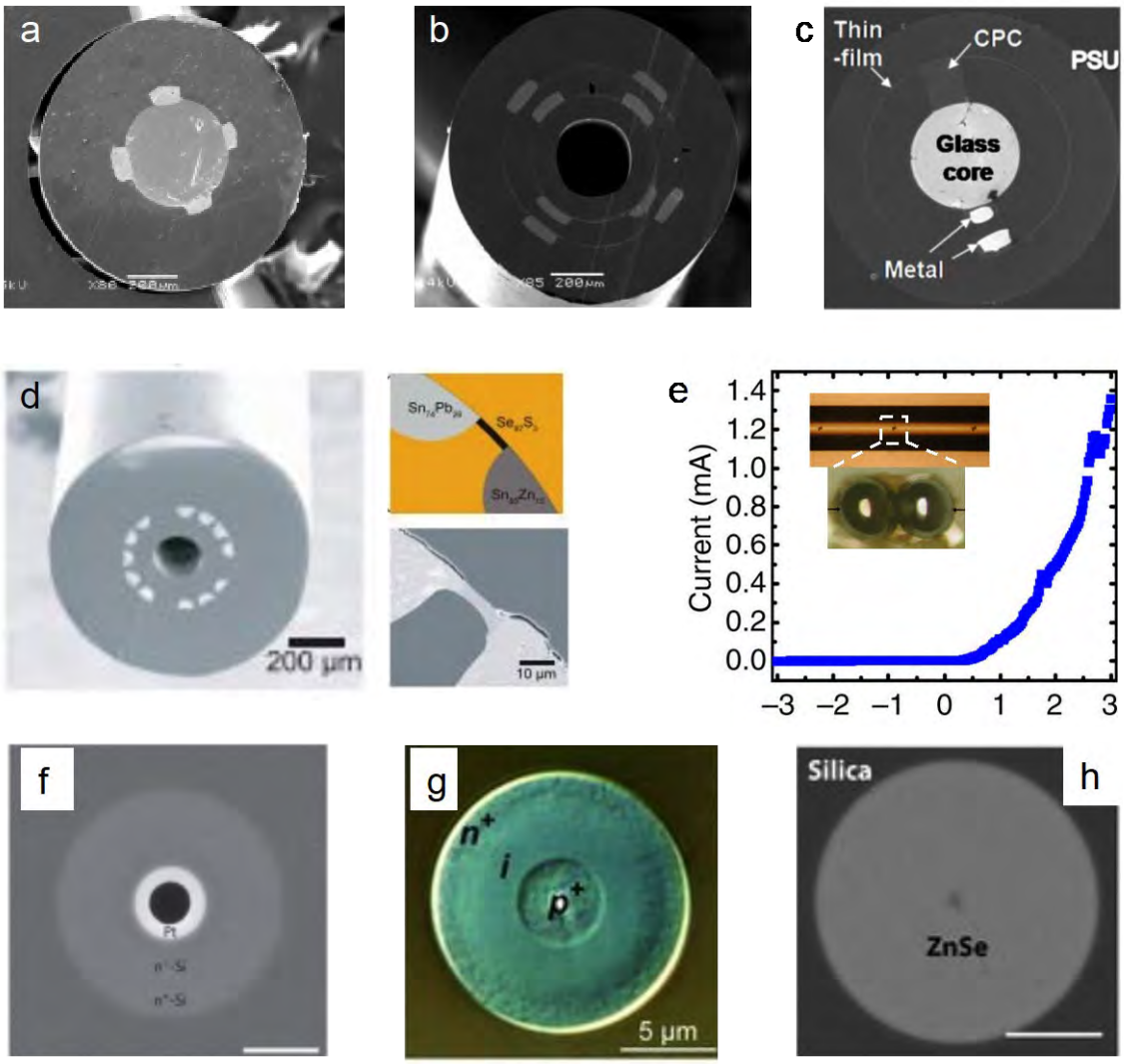

Figure3. a) Metal–insulator–semiconductor optoelectronic fiber. Reproduced with permissions.[7] Copyright 2012, Nature Publishing Group. b) Multi-junction fiber. Reproduced with permissions.[8] Copyright 2009, American Chemical Society. c) Axially symmetric photodetecting fiber that can distinguish optical illumination distributions. Reproduced with permissions.[9] Copyright 2010, OSA. d) Photodiode fiber. Reproduced with permissions.[10] Copyright 2011, National Academy of Sciences. e) P-N junction fiber formed via in-fiber capillary instability. Reproduced with permissions.[11] Copyright 2013, Springer Nature. f) Pt/n-Si Schottky junctions. Reproduced with permissions.[12] Copyright 2013, WILEY-VCH Verlag GmbH & Co. KGaA, Wein-heim. g) p-i-n junction fiber. Reproduced with permissions.[13] Copyright 2012, Springer Nature. h) ZnSe optical fiber. Reproduced with permissions.[14] Copyright 2011, WILEY-VCH Verlag GmbH & Co. KGaA, Wein-heim

core have also been co-drawn with phosphate glasses for optoelectronic and optical applications. [89][90][91] Another example of a thermally drawn optoelectronic fiber is shown in Figure 3c where a combination of metallic and polymer composite electrodes on the one hand, and of semiconducting core and thin-film architectures on the other, were used. This approach enabled to break the fiber axial symmetry through the construction of a convex electrical potential along the fiber axis thanks to the low conductivity of the composite compared to the metal. [75] The localization of an illumination point along a one-meter

photodetecting fiber with a sub-centimeter resolution was achieved. Finally, the integration of homo- and hetero-junctions that enable non-linear rectifying behavior was also demonstrated.[92][93] In Figure 3d we show a fiber with a Se-based thin film in contact with a SnZn electrode. As discussed in more details in Section 3, a ZnSe compound formed during drawing which created a hetero-junction with Se within the fiber.

The development of optoelectronic fibers within polymer matrices has triggered another research direction to integrate more conventional optoelectronic materials such as silicon (Si) in a fiber form. The drawing of semiconducting fibers integrating Si, Ge or various compounds precedes this effort and was originally concerned with extending the transmission bands to other wavelengths ranges, and integrate stronger non-linear effects. [94][95] Because of the much higher melting point of these crystalline semiconductors, silica cladding fibers, drawn at around 2000 ºC, are favored. For optoelectronic applications, it is necessary to find appropriate electrodes to interface with the semiconducting domains. At such high temperatures, and given the low viscosity at which crystalline materials are drawn, maintaining the interface between the semiconductors and the electrodes during direct thermal drawing remains a significant challenge. The first approach to alleviate this difficulty was to connect the materials post-drawing at the fiber ends rather than along the fiber axis. A recent approach to addressing this challenge relies on selective breakup of the semiconductor core and built-in electrodes via in-fiber capillary instability, as discussed in Section 4. [96][97] In Figure 3e we show the simultaneous capillary break-up of a p-type and a n-type domain that results two spheres in contact that exhibited an electrical response characteristic of a homo-junction (see section 4).

Another strategy for the monolithic integration of metals and semiconductors in fibers is to exploit the HPCVD technique. As different materials can be deposited sequentially, many devices such as ohmic contacts, p-n junctions, Schottky junctions, and p-i-n junctions can be fabricated. The creation of Pt/n-Si Schottky junctions via HPCVD was first demonstrated by He et al.[98], as shown in Figure 3f. The junction had a barrier height of 0.8 eV and exhibited a 3 dB bandwidth of up to 3 GHz at a wavelength of 1,550 nm, enabling high-speed photodetection at telecommunications wavelengths. [98] Polycrystalline silicon p-i-n junctions were then realized over a one-meter length of silica microstructured optical fiber, as shown in Figure 3g. These fibers exhibited a 3 dB bandwidth of up to 1.8 GHz when illuminated over a length of 1 mm and 100 MHz waveguide photodetection at 1064 nm. [99] The higher quantum efficiency makes them favorable for both photodetecting and photovoltaic applications. A one-cm p-i-n fiber electrically contacted on both ends exhibited an overall conversion efficiency of 0.5% under air mass 1.5 solar illumination. A recent work showed an improved conversion efficiency of up to 3.6% for a radial-junction solar cell fiber. [100] In Figure 3h we show another example of a semiconductor fiber with ZnSe this time fabricated via HPCVD [101]. While this fiber was designed for optical applications, it also paves the way towards optoelectronic functionalities as discussed above.

The short review of electronic and optoelectronic fibers highlight the significant potential of integrating complex functionalities within the confined and elongated space of polymer and glass fibers. In recent years,

several scientific and technological breakthroughs have enabled to improve fiber-based devices in three directions that represent the three pillars for high performance electronic and optoelectronic devices: the range of different material properties that can be exploited, the materials architectures and achievable feature sizes, and the materials microstructures.

3. Novel materials for the multi-material fiber platform

A major research effort in recent years has been put into looking for novel materials that could be either thermally co-drawn or integrated within micro-structured fibers. We distinguish here three approaches: searching materials with better functional properties that are usually processed at higher temperatures within phosphate or silicate glass claddings; low temperature electronic polymers with improved properties; and the ability to control the formation of materials during thermal drawing.

3.1 High temperature materials and thermoelectric materials

While good performance and several applications can be realized using polymer fibers integrating Se and other chalcogenide glasses compositions, high performance electronic and optoelectronic functionalities are conventionally obtained with crystalline Silicon, III-V and II-VI alloys, or other crystalline compounds. As discussed above, crystalline materials will melt during the drawing process and thick-walled glass tubes are needed as supporting scaffolds that contain and restrict the flow of the low-viscosity core crystalline materials. Despite the wide range of successfully drawn high-temperature semiconductors reviewed above, [102][103][104] there are several other interesting compound semiconductors that have recently been successfully drawn into fiber cores, which significantly broadens the range of potential applications.

Firstly, a phosphate glass-cladded fiber comprising a crystalline binary III-V semiconductor indium antimonide (InSb) core has been fabricated. [105]. Even though the InSb core is highly crystalline with some oxygen and phosphorus diffusing in from the glass cladding, such binary semiconductors may offer the possibilities of fiber-based nonlinear devices as well as the development of new in-fiber electronic or optoelectronic devices in the near future. Secondly, silicon-germanium (SiGe) in the fiber core extends the accessible wavelength range and the potential optical functionality because both the bandgap and optical properties can be tuned by changing the SiGe composition. Recently, the fabrication of SiGe-core fibers and the use of laser irradiation to recrystallize the core have improved the optical transmission properties. [106] Moreover, tailoring the recrystallization conditions allows the formation of long single crystals with uniform composition, as well as the fabrication of compositional microstructures such as gratings within the fiber core, as discussed in section 5.3.

Thirdly, inorganic thermoelectric materials have been thermally drawn into flexible fiber-like devices, as shown in Figure 4a. The resulting thermoelectric fibers are intrinsically crystalline, highly flexible, ultralong, and mechanically stable, while maintaining high thermoelectric properties similar to those of their bulk counterparts. The thermal drawing method works for a broad range of accessible thermoelectric materials such as bismuth telluride (Bi_2Te_3), chalcogenide glasses, tin selenide (SnSe), and SiGe with different

processing temperatures from 400 °C to 2000 °C. [107–109] Furthermore, two types of thermoelectric generators covering different curved surfaces are demonstrated to provide an mW/cm^2-level output power density, which is the highest level thus far achieved among flexible and wearable thermoelectric devices. [108] Additionally, a wearable two-dimensional active-cooling textile was assembled using thermoelectric fibers and a maximum cooling of 5 °C has been achieved, as we discuss in section 6). These fibers can be further woven into fabrics, which makes them particularly suitable for applications including green buildings, industrial energy management, wearable electronics, smart fabrics, and large-area sustainable energy generation systems.

3.2 Polymers and polymer composites

The ferroelectric and piezoelectric properties of some polymers such as polyvinylidene fluoride (PVDF), have been exploited for some time to create piezoelectric fibers capable of acoustic transduction.[40,80]The same types of materials were recently employed by Khudiyev et al. to fabricate electrostrictive fibers.[110] Electromechanical actuation under a DC voltage can make such fibers bend or deform with over 8% strain (see Figure 2c). This novel material opens interesting perspective to move and stir fibers for example in surgery situations. Lu et al. incorporated piezoelectric BTO or PZT nanoparticles (with concentrations of 20 wt%) or carbon nanotubes (0.4 wt%) into PVDF to improve its piezoelectric properties. [111] The piezoelectric PVDF nanocomposites were sandwiched by carbon-loaded polymer layers to create piezoelectric fibers as described in section 2.1.

As reviewed above, carbon-loaded polymers enable the inclusion of relatively thin and high aspect ratio electrically conductive layers that can serve as electrodes in different configurations. [40][97] This

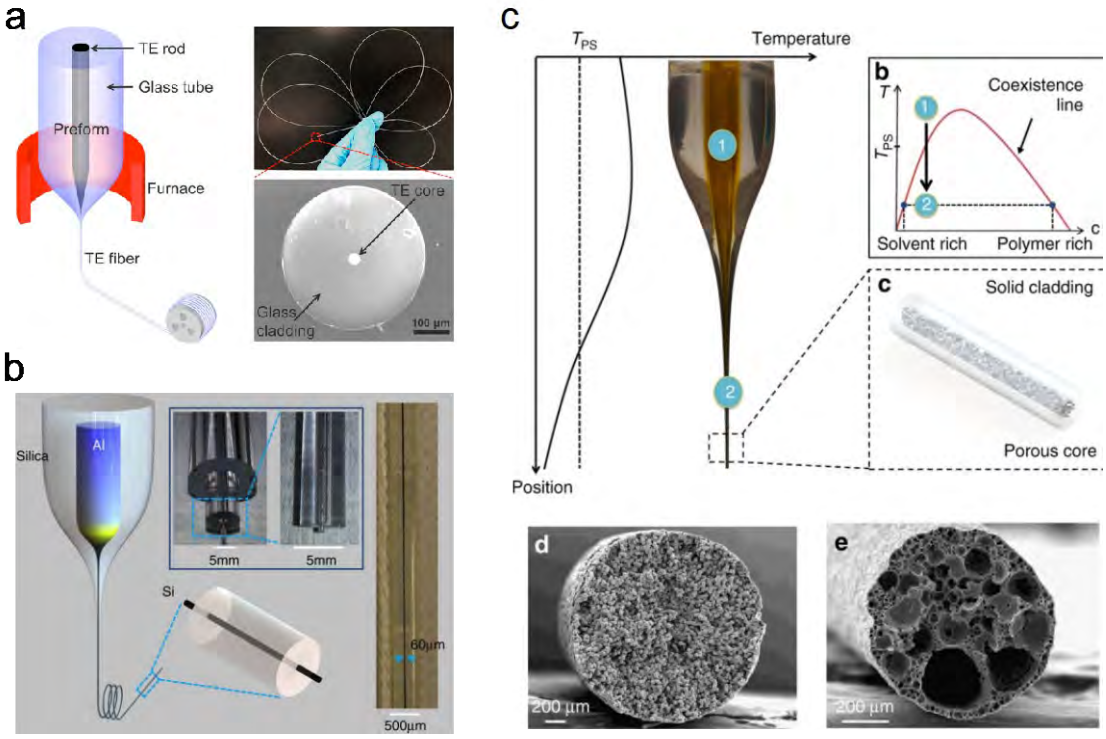

Figure 4. a) Thermal drawing of thermoelectric fibers. Reproduced with permissions.[15] Copyright 2017, Elsevier. b) Silicon core fiber drawn from aluminium-core-silica-cladding preform. Reproduced with

permissions.[16] Copyright 2015, Springer Nature. c) Thermally-drawn fibers with spatially-selective porous domains. Reproduced with permissions.[17] Copyright 2017, Springer Nature.

cannot be achieved with regular metals, which are drawn in the liquid state and would undergo capillary break-up during drawing. Until recently, carbon-loaded polymer composites had carbon black as a filler. Another carbon-based nanocomposite was recently demonstrated to be compatible with thermal drawing by Guo et al.. [112] In this study, carbon nanofibers (CNF) were incorporated in a polymer already loaded with carbon black. This improved the conductivity by two orders of magnitude, to reach 20 S/m, which enabled the use of such composites in advanced neuron-interfacing probes as we discuss in the last part. Finally, utilizing iterative size reduction by thermal drawing and the capillary instability of liquid wires, metal-polymer nanocomposite fibers were created by Lin et al. with Sn nanoparticles dispersed in the PES polymer. [113]

3.3 In-fiber synthesis of new materials during drawing

Another elegant approach that has been proposed in recent years consists in relying on the thermal process to bring together materials to react and form a new compound. The first fiber draw synthesis reported described the formation of high-melting point ZnSe in situ during a low-temperature thermal drawing (see Figure 3d). [93] It was discovered that drawing a polymer preform encompassing a thin layer of $Se_{97}S_3$ alongside $Sn_{85}Zn_{15}$ metallic electrodes yielded electrically contacted crystalline ZnSe domains at the interface between the metallic elements and the selenium-based layer. The fiber device exhibited a rectifying behavior, due to the large discontinuity in the valence band at the $Se_{97}S_3$/ZnSe interface. The noise-equivalent power of this device was 1000 times lower than previous multi-material thin-film photodetecting devices. [93] This reaction, however, was limited only to the surface of the electrode, while the bulk was not utilized. Replacing the Zn-based electrode with a thin film of pure Zn that mechanically broke up during drawing on top of the Se-based layer significantly increased the volume of ZnSe formed. This work also provided direct atomic-level compositional and structural analysis of the ZnSe and experimentally probed the thermodynamics and kinetics of the compound formation. [92] Another chemical reaction during thermal drawing was observed in the high-temperature silica platform. When drawing an aluminium rod cladded by a silica tube, the Si atoms in the silica diffused into the aluminium core forming a high-quality crystalline Si core, [114] as represented in Figure 4b The Si core formation mechanism can be rationalized as follows: (i) Al reduces the surrounding Al_2O_3, releasing, Si atoms, O^{2-} and Al^{3+}. All the products dissolve in the molten Al; (ii) Si atoms remain in the molten Al due to their miscibility, whereas O^{2-} and Al^{3+} form Al_2O_3, precipitating out of the molten Al; (iii) molten Al-Si floats up and molten Al_2O_3 sinks to the bottom due to a high density contrast; (iv) Al in the Al-Si melt is consumed gradually, leaving less and less Al_2O_3; (v) Finally a Si melt is achieved at the top of the core. The Si core is purified by virtue of a zone melting condition established by the temperature profile in the furnace. This kind of understating constitutes a significant advancement in

exploiting chemical reactions and density contrasts to separate species and form novel compounds or pure materials.

Another class of materials that had been disregarded until recently because of the difficulty to control their microstructure during thermal drawing are porous materials. Porous polymer fibers are typically fabricated by the extrusion or spinning of a polymer solution with complex spinnerets,[115] electrospinning an emulsion system followed by a calcination process, [116] or thermally-induced phase separation in the fiber during electrospinning. [117] These fibers find intriguing applications in catalysis, [118] sensors, [118] water absorption, [118] gas separation, [119] and tissue engineering. [120] Grena et al. [121] demonstrated that spatially-selective porous fibers can be fabricated by employing phase separation of polymer solutions into a solvent-rich and polymer-rich phase during thermal drawing, [121] as illustrated in Figure 4c. Besides the typical criteria set for materials selection, additional constraints on the materials for the fabrication of porous fibers via thermal drawing are as follows: the solvent should not dissolve the cladding materials; the solution should not boil at the drawing temperature; and the solution should exhibit phase separation. Due to various designs of the preform, such porous fibers exhibit complex external geometries such as triangular, cross-shaped, or core-shell. Pore size tunability between 500 nm to 10 μm were achieved by controlling kinetics of phase separation. In addition, multiple materials can be incorporated adjacent to the porous domain creating unique functionalities in fibers. In particular, the authors demonstrated that conductive materials interfacing these porous fibers allowed for the measurement of the ionic conductivity of an electrolyte filling in the porous domain. This work lays a solid foundation for the fabrication of fiber-based batteries or supercapacitors via thermal drawing. Furthermore, by judicious choice of materials and design of preform architecture, the authors were able to make fibers consisting of hollow core lined by porous domains as claddings. [122] Such fibers allowed neurites in the hollow core to grow fast and extend along the fiber length because nutrients could in principle diffuse into the hollow core directly through the porous cladding. This contrasts with hollow core fibers with a dense cladding where neurites exhibit a diffusion-limited growth mode and thereby resulting in a short extension path. [123] These fibers present excellent nerve guidance scaffolds and allow for accelerated nerve repair.

4. The fluid dynamics and rheology of thermal drawing

Once we can process a large variety of materials, the second pillar of advanced functionality resides in the ability to structure these materials in the right architecture and feature size. The deeper understanding of the thermal drawing process developed in recent years enables to fabricate fibers with more complex architectures, and shape materials at the desired geometry and scale to improve device performance and open novel application opportunities.

4.1 Controlling the shape and texture of polymer fibers

The controlled shaping and texturing of surfaces at the micro- and nanoscales is a powerful tool for tailoring how materials interact with liquids, electromagnetic waves, or biological tissues. The increasing scientific

and technological interest in advanced fibers and fabrics has triggered a strong motivation for leveraging the use of different fibers with different shapes and surface textures. The thermal drawing process is particularly attracting because of the scaling effect that occurs during the preform-to-fiber deformation that allows a direct 'top-down' fabrication to create micro- and even nanoscale patterns from a macroscopic preform. Recently, a deeper understanding of the fluid dynamics during drawing has enabled to control fiber shapes and textures at the sub-micrometer scale. The first example of such exploitation of thermally drawn fiber shape was reported by Banaei et al., who designed the cladding of optical fibers as luminescent solar concentrators. [124] Next, Yildirim et al. demonstrated star-shaped cross-sectional fibers made of polyetherimide (PEI), with the feature-size of the star spikes as small as 30 μm; [125] these star-shaped fibers then were employed as hydrophobicity-enhancement surfaces or as microfluidic switches. A similar approach using thermal drawing of textured preforms made of PEI reported by Koppes et al., allowed the fabrication of 50 μm

micro-grooved hollow-core fibers, which were used as nerve guiding conduits to study the effect of micro-groove size on axonal growth direction and acceleration. [123]

While the concept was opening novel opportunities for fiber-based devices, fiber-processing techniques have exhibited an inherent limitation due to the smoothing out of small surface roughness induced by polymer reflow. This has limited the feature sizes of textures achievable at the fiber level to tens of micrometers, significantly restricting their possible use. Indeed, during the drawing process, curved surfaces with relatively high interfacial tension will undergo thermal reflow driven by Laplace pressure, leading to a smoothing out of small textures that gets increasingly faster as the pattern size gets smaller. This reflow during drawing was recently experimentally analyzed and modeled. [126] It was found that the characteristic time of the reflow deformation, τ, is proportional to the feature size λ of the surface pattern and the viscosity of the material γ, and is inversely proportional to its surface tension γ: $\tau \sim \frac{\eta \lambda}{\gamma}$. In order to realize surface patterned fibers with micrometer and sub-micrometer feature sizes, which are required for many applications in optics, optoelectronics, biology and bioengineering, an original approach was proposed where during the preform creation, the polymer with the desired textured surface was interfaced with a sacrificial material to reduce significantly the interfacial tension. This in turn reduced the Laplace pressure that is driving the reflow, and consequently enabled the fabrication of submicrometer patterns of various sizes and shapes on the external surface of flat ribbons or on the highly-curved internal surface of hollow-core fibers. [126] In Figure 5a, we show a graph that represent a theoretical reflow factor versus the size of targeted textures at the fiber level. This factor was extracted from the modeling of the polymer texture reflow during drawing based on a Navier-Stokes formalism. A large reflow factor is associated with a loss of texture at the fiber level as can be seen on the top

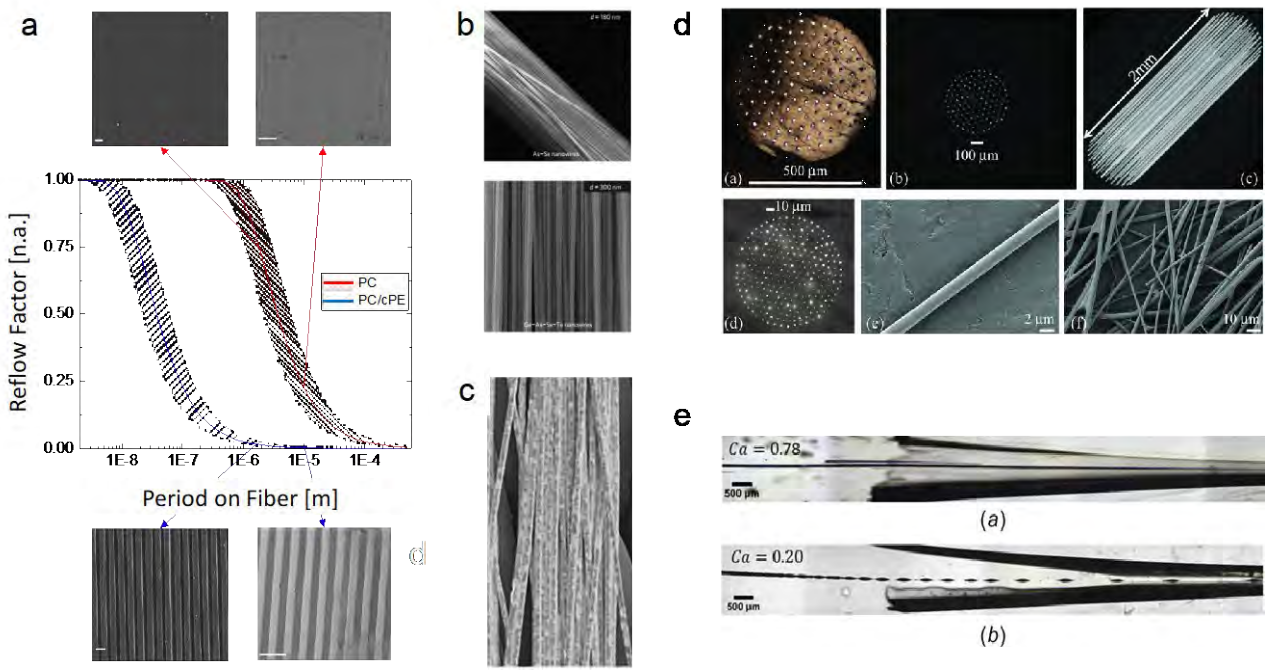

Figure 5.

SEM micrographs that show the top view of a polycarbonate (PC) fiber drawn out of a textured preform (red curve). The blue curve on the other hand corresponds to a textured PC preform drawn in contact with a carbon black loaded polycarbonate (PC) cladding. The interfacial tension between PC and CPC is drastically reduced compared to bare PC, which shifts the reflow factor curve and enables to maintain texture with sub-micrometer feature sizes as shown in the bottom SEM micrographs. It was demonstrated that such textured fibers open significant opportunities for applications in fibers and textiles with tailored surface properties, fibers with photonic effects, or scaffolds for the growth of neuron-like structures. Submicrometer surface-patterned fibers were independently obtained by Khudiyev et al. using a similar approach, [127] which confirmed these experimental and theoretical findings. This development contributes to a deeper understanding of the preform-to-fiber deformation process and provides exciting opportunities for applications in various fields such as healthcare, bioengineering, electronic textiles, or optoelectronics, as we discuss further in Section 6.

4.2 Continuous conducting and semiconducting fiber-integrated wires

Maintaining not just polymeric but also micro-structured conducting and semiconducting domains along fibers is also subject to intense research. It is a key aspect in order to improve the performance and open fiber devices to new functionalities. It also brings novel insights into the fundamental driving force of stability versus break-up in thermally drawn structures. Several groups have studied the stability of micro- and nanowires and the attainable feature sizes in recent years, again from a fluid dynamics perspective. Deng et al. considered the structure used in photonic bandgap fibers, which consists of a concentric cylindrical-shell multilayer structure. [128,129] When the glassy selenium shell becomes too thin, it was

observed to break up into nanosized filaments in the polymer matrix. Thanks to a model based on the Navier-Stokes formalism and finite-element simulations of the instability process, an instability timescale was extracted for various viscosity ratios and feature sizes. This yielded stability maps that can help materials selection for fibers containing thin layers. This pioneering work in the understanding of the interplay between viscosity and surface tension to analyze the break-up of thin films set the basis for a deeper understanding of the achievable feature sizes and architectures via thermal drawing. It also explained the smoothing out of Rayleigh instabilities along the drawing direction, preventing their growth and hence explaining the extremely long nanowires that could be achieved. Other authors put these principles into play by generating nanowire arrays by iteratively drawing several times macroscopic rods encapsulated by a cladding material. For example, starting with a 10 mm rod, chalcogenide glass nanowire arrays could be created in a polyetherimide matrix, [48] as can be seen on the SEM micrographs of Figure 5b. This can also be applied to core-shell nanowires. [130] Furthermore, a post-drawing heat treatment of the fiber enables conversion of the nanowires into nanospheres, and also intermediate nanostructures such as short nanorods and even nanosprings, which are non-axisymmetric. [130]

Nanosized wires can be fabricated when they are processed at high viscosity that slows down capillary break-up effects. Materials such as metals and alloys that melt during fiber drawing are processed at low viscosity which limits the achievable feature sizes. Recently, a series of publications have focused on understanding and exploiting the fluid dynamics effects behind the drawing of metals in the molten states within a viscous polymer cladding. By proposing an interpretation taking into account shear stress experienced by the molten metal, Yaman et al. could rationalize reaching continuous metallic wires with 4 μm in diameter. [48] Similar diameters were obtained by Zhao et al. for Sn wire inside a PolyetherSUlfone (PES) cladding as shown in Figure 5c, before observing capillary break-up and the formation of Sn nanoparticles.[131] Next, Xue et al. used a numerical model with the software PolyFlow to explore the impact of various factors on the capillary instability, and concluded that a fast, cold drawing process and a thin cladding are preferable. [132] Due to the limited diameters achievable with metallic microwires, arrays of the latter cannot lead to metamaterials that would interact with visible light. However, applications from the terahertz through the edge of the mid-IR ranges were demonstrated, optimizing the process and making it possible to achieve metallic wires as small as 1 micron in diameter (see Figure 5d). [133] Zhao et. al. recently proposed a new long wavelength model that brings new insight in the drawing of metallic core in the molten state via thermal drawing. They estimated a critical dimensionless capillary number above which continuous Sn microwires can be created in PES fibers. [134] In Figure 5e we show how this transition can be observed experimentally with a continuous (a) to a breaking-up (b) wire as the capillary number is lowered. Such recent analysis is participating in the deeper understanding of the fluid mechanics at play during multi-material drawing.

4.3 Micro- and nanoparticle based fiber devices

Understanding and controlling interfacial effects to exploit reflow or break-up to design different surface textures or micro-wires have been a key recent development to structure materials at the sub-micrometer scale. It appears in recent years that exploiting capillary break-up effects at the fiber level can also lead to intriguing phenomena and applications. In particular, the realization of in-fiber particles via the Plateau-Rayleigh capillary instability (PRI), has been at the heart of intensive research. This process typically begins with a macroscopic composite multi-material solid-state preform drawn into a fiber that is subsequently heated to induce dynamic in-fiber fluid instabilities at the heterogeneous interfaces along its entire length. Subsequent quenching produces a necklace of particles suspended in the solid matrix constituting the fiber cladding, as depicted schematically in Figure 6a. [135] As this fabrication approach relies on a physical break-up mechanism that results from the interplay between surface tension and the viscous dissipation force between the molten fiber cladding and core, it significantly broadens the repertoire of accessible materials and geometries compared to conventional chemical synthesis.

Fabrication of in-fiber particles has been achieved by softening the pre-fabricated fibers either by isothermal heating via furnace[96,97,136–141] or by axial thermal gradient heating via oxyhydrogen flame or furnace. [135,142,143] However, these approaches face some challenges, such as wide and uncontrollable heating profiles, unavoidable satellite particle generation, and limited selection of functional materials, which have limited their study and possible applications. To address these limitations, as an ideal heating source in the thermal treatment, a CO_2 laser has been recently applied to control the in-fiber fluid dynamic unstable area. [144,145] Due to the small area heated by the laser beam, only a short section of fiber reaches a temperature sufficient to melt both the fiber core and cladding. Then, a perturbation occurs at the molten core/cladding interface, leading to a transformation from a continuous cylinder to a chain of spherical particles with uniform diameters. More importantly, by changing the feed-in velocity v_f, particles with different diameters can be fabricated from the same fiber, thus the amplification ratio can be controlled. Furthermore, laser heating offers a stable and widely tunable in-fiber temperature profile through adjusting the radiation power according to the actual absorption ratio of different materials.

A broad range of functional materials has been selected to construct in-fiber particles in low-, middle-, or high-temperature regions, with the corresponding cladding materials of polymer, soft glasses, or

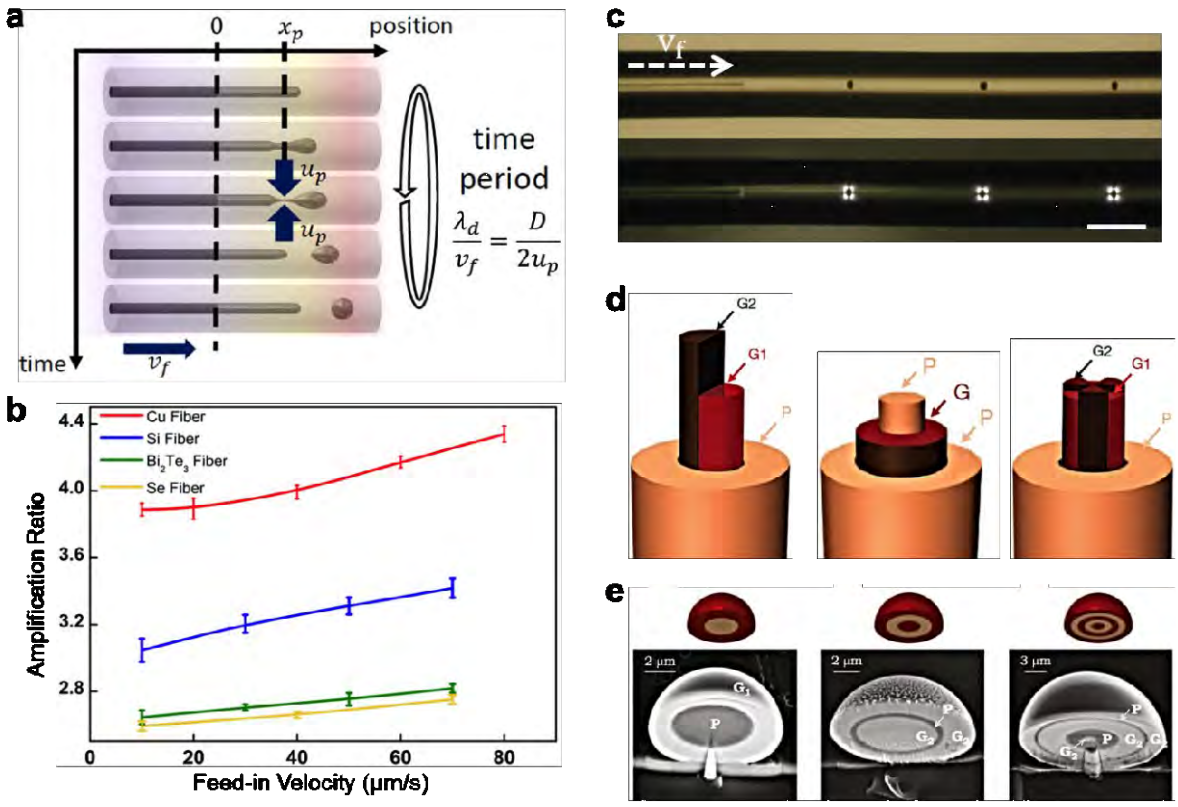

Figure 6. a) Step-by-step formation of a particle and dimensional analysis: in the time it takes to go over one full cycle of particle formation, in which a length λ_d is fed at speed v_f, the core of diameter D is pinched at a speed up. Reproduced with permission.[11] Copyright 2013, Springer Nature. b) Amplification ratio as a function of the feed-in velocity v_f for selected multi-material fibers. Reproduced with permission.[18] Copyright 2017, WILEY-VCH Verlag GmbH & Co. KGaA, Wein-heim. c) Top: A section of the fiber resulting from the break-up process via axial thermal gradient heating, including a continuous silicon-core followed by broken-up particles as observed under a transmission optical microscope. Bottom: The same sample is placed between crossed polarizers. Azimuthally fourfold stress fields of the silicon-particles are evident. (Scale bar: 100 μm). Reproduced with permission. [19] Copyright 2017, National Academy of Sciences. d) Schematic of various fiber structures: Janus, core-shell, and 'beach ball'. G: glass, and P: polymer. Reproduced with permission. [20] Copyright 2012, Springer Nature. e) Control over particle structure in the radial direction. G: glass, and P: polymer. Reproduced with permission.[21] Copyright 2016, National Academy of Sciences.

fused quartz. These functional materials typically include semiconductor, electric, and chalcogenide glass materials with different melting temperatures from 400 K to 2400 K and 10 orders of difference in fiber core/cladding viscosity ratios, as shown in Figure 6b. [144] Local material engineering can also be achieved via the compressive stress induced by heating and subsequent controlled cooling, as shown in Figure 6c. [143] It is possible for more than two materials to be incorporated in the same fiber, which enables the construction of multi-material structured particles such as bi-compartmentalized Janus particles formed of two hemi-particles from different materials, core-shell particles, and 'beach ball' particles, as illustrated in Figure 6d. [136] By actively controlling the viscosity contrast between different materials within a single fiber,

more complicated particle structures have been demonstrated such as multi-material photonic particles with the precise allocation of high refractive-index contrast materials at independently addressable radial and azimuthal coordinates within their 3-dimensional architectures, as shown in Figure 6e. [140]

The recent deeper understanding of sphere break-up within multi-material fibers opens a new playing field for fluid dynamics that enables the interaction between different materials in the context of fiber thermal drawing with geometries and other parameters that are not accessible in traditional platforms. This work will enable applications including electronic devices, photovoltaics, medicine and health-care, targeted drug delivery, biology, chemical sensing, and cosmetics.

4.4 Revisiting the selection of materials for thermal drawing

The fluid dynamic analyses described above have in large part consisted of investigating the interplay between viscosity and surface tension. Until now however, the field of thermal drawing has not considered having a deeper look into the rheological dynamics that govern the overall value of the viscosity. Despite the existence of general guidelines regarding required viscosity values, the lack of a deeper understanding of the materials properties that govern their ability to be thermally drawn is hindering the expansion of both the choice and combination of materials that could be processed by the thermal drawing technique. Consequently, the range of structures and functionalities that could be achieved is limited as well.

Recently, a deeper understanding of what could constitute good cladding materials in the context of multi-material thermal drawing has been proposed. Qu et al. used punctual rheological and microstructural analyses to discriminate among thermoplastics and thermoplastic elastomers those that could be thermally drawn, with the aim of fabricating, for the first time, highly elastic functional fibers via thermal drawing. [56] Through the exploitation of oscillatory shear rheology of commonly used thermoplastics for thermal drawing, such as polycarbonate (PC), they observed that a flow in the viscous regime at high viscosities can be better defined as a temperature window, where the loss modulus G’’ changes slowly with temperature, crossing over the elastic modulus G’ that rapidly decreases. Therefore, they state that a transition from an elastic to a viscous regime, with a dominating

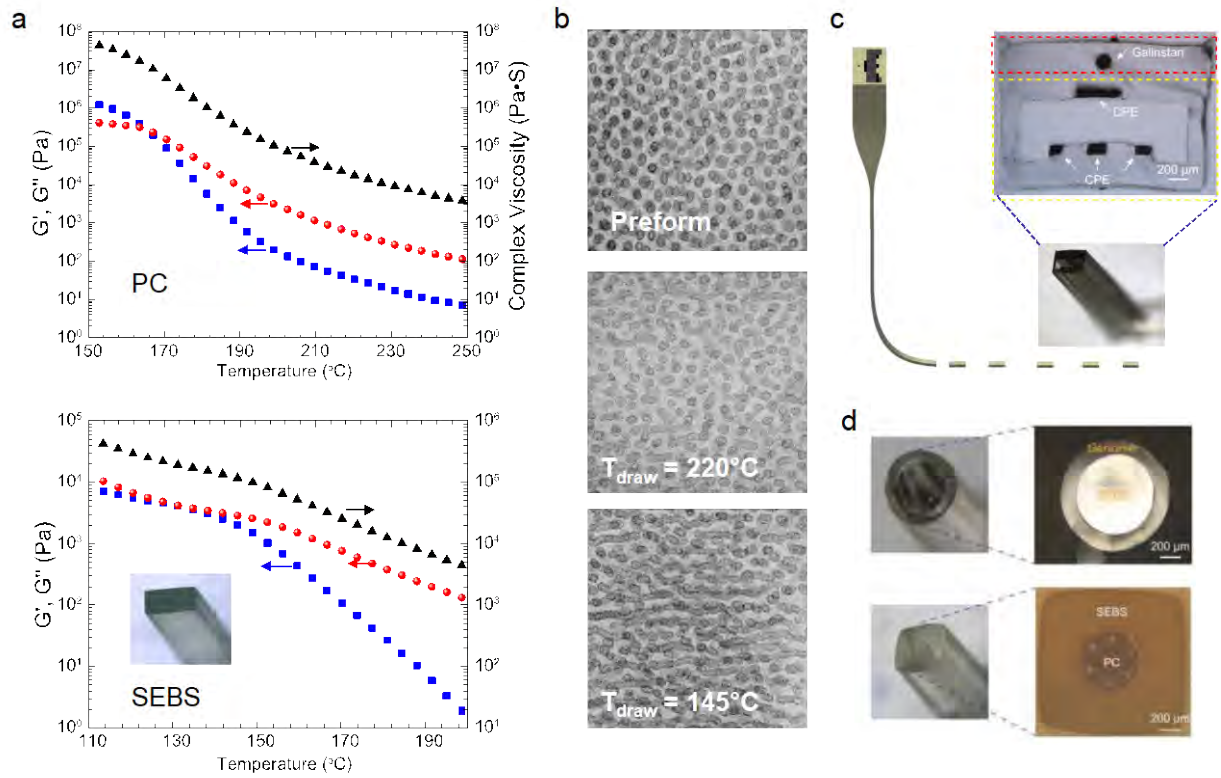

Figure 7

loss modulus that changes slowly with temperature, a good rheological signature for a material to be processed at high viscosity during thermal drawing.

This rheological criterion to discriminate materials has expanded the range of materials that can be considered for thermal drawing. Figure 7a compares rheological properties of PC and a high molecular weight poly(styrene-b-(ethylene-co-butylene)-b-styrene) (SEBS). They both satisfy the above rheological requirements and could be successfully drawn. To elucidate the drawing effect at the micrsoctructure level, In Figure 7b we show the TEM images of SEBS before and after drawing at two different temperatures. It appears that at the preform level, the PS spheres (in black) are dispersed randomly in the elastic EB block matrix (which was confirmed from a SAXS analysis in the same study). At the fiber level, however, the TEM analysis reveals an elongated cylindrical morphology for the hard phase on top of the original sphere-like domains, more pronounced as the fiber is pulled at a lower temperature. PS domains seem hence not to deform excessively but rather to be sheared and aligned by the movement of the EB block chains in the neck-down region during drawing. The hard phase aggregates in the fiber can ensure physical cross-linking as the material returns to room temperature, which preserves the elastomeric-like mechanical attributes of the material after drawing.

In the same study, the authors also report two examples of materials that are not suitable for the thermal drawing process: a copolymer of polycarbonate and polyurethanes (PCU), and a SEBS grade with a lower molecular weight and higher polystyrene content, neither of which. In fact, the PCU exhibited G' and G'' moduli that quickly decreased with temperature, while the second kind of SEBS had a G' that remained higher than G'' thus breaking during pulling without deforming plastically in the viscous regime. Certainly,

shear viscosity alone does not capture the complexity of the thermal drawing process, and many other parameters should be taken into consideration such as the role of extensional viscosity or shear thinning phenomena. Nevertheless, this study allows identification of a more in-depth requirement for discriminating the drawability of materials. All the materials that meet this criterion for shear viscosity reveal a microstructure and flow mechanism compatible with the thermal drawing process. This is opening the way to the selection of novel materials and applications for electronic and optoelectronic fibers. For example, in the described study, the identified thermoplastic elastomers were used as cladding to encapsulate complex hybrid architectures to realize soft and stretchable electronic devices and optical fibers. In Figure 7c, we show an architecture that integrate a liquid metal electrode (Galistan), and three carbon black loaded polyethylene electrodes separated from a fourth one by a hollow channel. This fiber can sense and measure pressure, while discriminate compression versus shear mechanical deformation. Figure 7d shows two types of thermally drawn stretchable optical fibers, a step index one (top) made out of two elastomers, and a hybrid thermoplastic – elastomer one (bottom). The opportunities opened by this novel processing of thermoplastic elastomer is further discussed in Section 6.

5. Microstructure Engineering of Functional Materials

Now that a variety of materials can be thermally drawn within increasingly complex architectures, the last pillar that links the processing to the performance of the targeted device is the material microstructure. Besides the work on the compatibility with thermal drawing of some thermoplastic elastomers described above, the state of the microstructure of materials after drawing and its influence on the fiber device have been studied only for semiconducting materials. In multi-material polymer fibers, both as-drawn chalcogenide semiconductors made via the thermal drawing approach, and deposited semiconductors in glass tubes made via HPCVD exhibit an amorphous state. Amorphous semiconductors have a disordered structure that is detrimental to their electronic and optoelectronic applications. In recent years there has been tremendous efforts put into understanding and controlling crystallization of amorphous semiconductors in the confined space of micro-channels within micro-structured fibers to improve the device performance and expand their applications.

5.1 Furnace-based thermal annealing

The simplest and most straightforward way to induce crystallization is to anneal the fibers in a furnace above the glass transition temperature of the semiconducting materials. For example, the first metal-semiconductor thermally drawn fiber with crystallized domains was obtained by annealing an AsSeTe chalcogenide glass for several days at a temperature high enough to slowly induce crystallization, but small enough so as not to deform the fiber cladding. In Figure 8a we show the SEM cross section of a solid core AST glass connected by four tin electrodes. After annealing, clear crystals can be seen growing mostly from the crystalline electrodes, which were characterized via X-ray diffraction. In the same study, heat-treated field-effect fibers displayed a substantial increase in conductivity by three orders of magnitude compared to

the amorphous fiber after thermal annealing in a furnace. [82] Other optoelectronic fibers could exhibit high responsivity and low noise equivalent power (NEP) after thermal annealing, showing the capability of chemical sensing via chemiluminescence. [88] To further investigate the crystallization of chalcogenide glasses post-drawing, and control the location of crystallized domains, Yan et al. recently proposed a fiber-tip crystallization scheme using the furnace-based annealing approach for making high-performance photodetecting fiber probes. [146] In Figure 8b we show the structure of the used fiber with a Se core in contact with polymer composite electrodes. Despite an improved photosensitivity, this method created a microstructure with small grains and a high number of grain boundaries that still impaired charge transportation. Heat diffusion also made it difficult to control the size of the crystallized domains.

Thermal annealing schemes have also been used to modify the semiconductor core in silica-cladded optical fibers. Gupta et al. exploited rapid photothermal processing to anneal glass-clad silicon optical fibers under an ultrahigh-purity nitrogen environment at 950 °C. [147] The annealed fiber exhibited improved local crystallinity, and single crystals with a length of nine millimeters were reported. Furthermore, the nature of the crystallographic orientation of the core material relative to the fiber axis and the influence of core geometry on the crystallography were investigated. [148,149] In another study, multi-step annealing of the amorphous silicon core below its melting point in a silica optical fiber was reported. It allowed for an increase in the polycrystalline grain size and a decrease in the dislocation defects. [150] A similar annealing method was also employed in order to crystallize the amorphous Se core in phosphate glass fibers. [91] The improved microstructure of these fibers resulted in a low optical loss, which was comparable to the loss in planar semiconductor waveguides configurations.

Although furnace-based thermal annealing is capable of inducing crystallization of amorphous semiconductors in a very simple manner, it is hard to control the heating and cooling rates as well as the thermal gradient. This approach therefore results in difficult control over material microstructure in terms of phase, grain size, crystallization volume, and crystallographic orientation. Nevertheless, we anticipate that more desired microstructures can be achieved by optimizing annealing strategies or fiber design, such as reducing the size of the semiconductor core to the range of grain size, [151] tapering optical fibers at temperatures above the melting point of the semiconductor, [152] and employing seed-mediated growth of single crystals by introducing foreign crystals.

5.2 Laser-based annealing

Another more versatile approach to induce crystallization relies on laser-based annealing. Laser light can accurately deliver high-density energy into a confined region thanks to a controlled and well-defined penetration depth. Heat generation during the laser treatment is thus limited to a smaller region, with typical penetration depth of visible light in commonly used semiconductors being a few tens to a few hundreds nanometers. [153] It can enable a better control over thermal gradient. Laser annealing was recently used for thermally drawn optoelectronic fibers by Yan et al.. [146] They exploited a visible laser to anneal amorphous Selenium in an optoelectronic fiber and demonstrated that the laser annealing scheme enabled a better

control over microstructure at the fiber tip. In Figure 8b, the cross-section of the Se core fiber can be seen, as well as the SEM micrograph of the cross-section after laser annealing. A polycrystalline structure can clearly be seen, revealed also by EBSD and TEM characterization. The average grain size reached a few microns in the direction perpendicular to the electrodes, which reduced the number of grain boundaries compared to a furnace annealing approach. Grains were also much smaller in the direction of the fiber axis, of the order of the light penetration depth, resulting in a shallow crystallization depth. Such an optimized microstructure led to excellent device performance. The photoresponsivity was much higher in a wide range of illumination powers and the photosensitivity was several orders of magnitude higher compared to that of fibers annealed with a furnace-based approach. Optimizing the incident power intensity, annealing time, and annealing steps is expected to further optimize the semiconductor microstructure with larger grains, controllable crystallization depth, as well as preferential crystallographic orientations. The laser annealing approach demonstrated here also has the potential to be applied in the longitudinal direction of the fiber by focusing the beam on the active material through the cladding. This would enable the ability to write, at any location along kilometer-long fibers, devices of controlled microstructure and performance. The small cross-section and large aspect ratio of the high-performance fiber also allows access to remote and confined environments where rigid and planar point photodetectors are unable to reach.

5.3 Laser-based solidification

The integration of high-melting point semiconductors such as Si, Ge, and SiGe bring significant scientific and technological opportunities for electronic and optoelectronic fiber devices. Both HPCVD within a microstructured fiber, and the direct thermal drawing provides a platform for the deposition of these semiconducting materials. The first technique results in high purity materials in the amorphous state, while molten core thermal drawing leads to polycrystalline semiconductors, both of these microstructures exhibiting high optical losses and poor optoelectronic properties. A high-power laser-induced solidification approach has recently been demonstrated as uniquely capable of tailoring the composition, crystallinity, and grain size thanks to the high control over the heating and cooling rates, and the thermal gradient. Coucheron et al. reported the fabrication of high-quality SiGe-core optical fibers with significantly improved optical transmission via thermal drawing followed by laser-melting post-processing. [106] During the CO_2 laser treatment, the silica cladding was strongly heated due to the absorbed infrared radiation and the SiGe core was melted through thermal conduction. By controlling the translation rate of the CO_2 laser, they were able to achieve a solidification velocity below the critical velocity predicted by the principle of constitutional supercooling, leading to microsegregation-free structures in the fibers. The rapid translation and the large temperature gradients also suppressed nucleation and growth of unstable nuclei, generating large single crystals as long as 7 mm, shown in the SEM micrographs in Figure 8c. The segregation of elements in the alloy system can be avoided, but it can also be utilized to create gradient composition structures. A compositional grating comprised of Ge-rich regions and Si-rich regions with the period of 40 μm was shown

by interrupting the laser beam momentarily. This work demonstrates that the silica glass cladding can serve as an efficient crucible for controlling

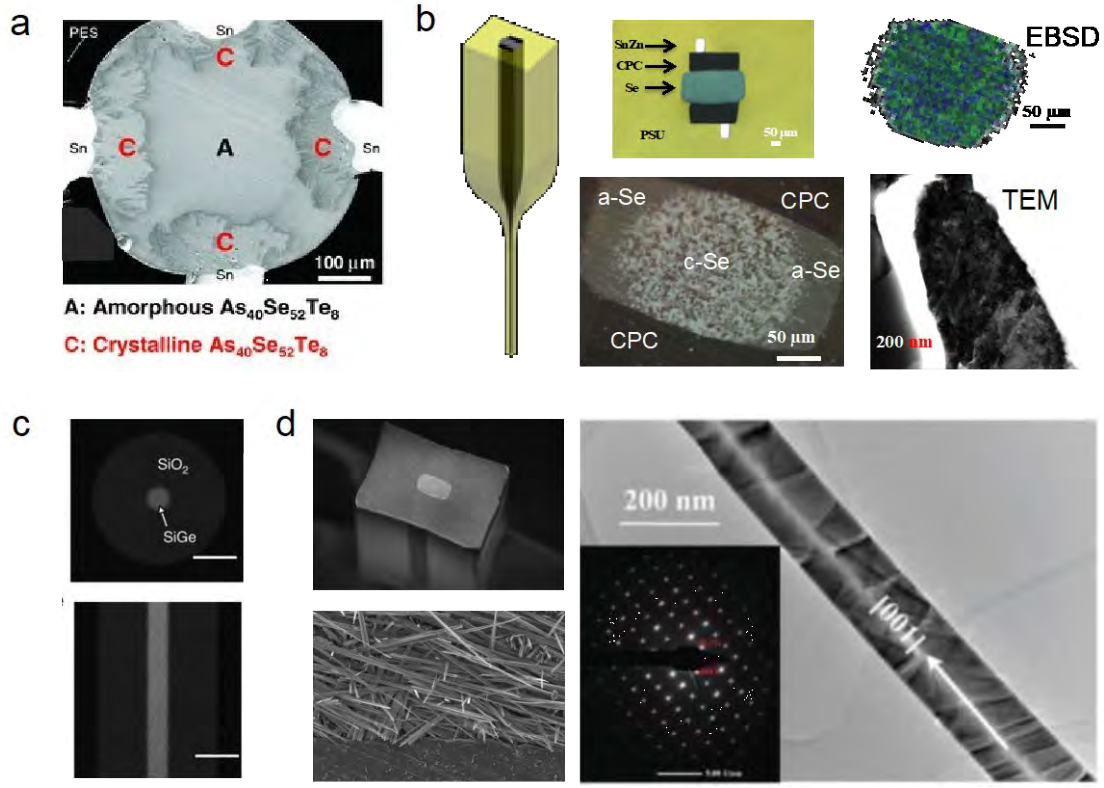

Figure 8. a) Crystallization of in-fiber AsSeTe chalcogenide glass via furnace-based annealing. Reproduced with permissions.[6] Copyright 2010, WILEY-VCH Verlag GmbH & Co. KGaA, Wein-heim. b) Crystallizaiton of Se in a photodetecting fiber. Reproduced with permissions.[22] Copyright 2017, OSA. c) SiGe single crystal in an optical fiber. Reproduced with permissions.[23] Copyright 2017, Springer Nature. d) Se nanowire-based optoelectronic fiber. Reproduced with permissions.[24] Copyright 2017, WILEY-VCH Verlag GmbH & Co. KGaA, Wein-heim.

material microstructure and elemental segregation and crystallographic structure of the core, thereby tailoring the optical properties of the fiber. From a fundamental point of view, this scheme provides a novel tool to re-investigate classic microsegregation-free mechanisms (the constitutional supercooling principle, the limit of absolute stability, and partitionless solidification). This technique is also applicable to other in-fiber materials. For example, Healy et al. used the same CO_2 laser as the radiation source to recrystallize the silicon core of optical fibers. [154] Fibers with single crystals over the entire scanned region that were as large as 1.8 cm were created. The optical loss was thus significantly decreased. Subsequently, Ji et al. employed a continuous wave laser treatment using above-bandgap radiation that only targeted the fiber core to remelt amorphous Si deposited in silica fibers. [155] The single crystal fibers, as long as 5.1 mm, exhibited a very low optical loss down to 0.47 dB/cm at the standard telecommunication wavelength and a superior photosensitivity comparable to bulk silicon.

The versatility of the laser-based solidification approach has also been illustrated for tailoring the microstructure of in-fiber SiGe spheres obtained via PRI. By precisely controlling heating and cooling rates, Gumennik et al., showed the creation of SiGe compositionally segregated Janus spheres and spheres of dendrites of Ge in Si in silica fibers. [143] Another appealing example is to modify the electronic band structure of in-fiber semiconductors via high stress introduced during the laser solidification process. Healy et al. employed a continuous wave visible radiation that passes the cladding and interacts with the core material to selectively melt the amorphous silicon core.[156]The unique fiber geometry allowed the crystalline silicon to be strongly confined within the silica cladding after solidification, imparting built-in tensile stress of up to 5 GPa in the silicon crystal lattice. It was observed that the bandgap was reduced from 1.11 eV down to 0.59 eV, enabling optical detection across the entire telecommunication band. Similar work further investigated how the laser shut-off rate that controls the cooling rate of spheres modified the stress/strain scenario in solidified silicon spheres. [145] These work further demonstrate that the confined fiber geometry is acting as a unique platform for the fabrication and fundamental investigation of novel electronic and optoelectronic devices with unusual properties.

5.4 Sonochemical synthesis

Another strategy to control the material microstructure is via the growth of semiconducting nanowires. This approach has not been exploited in the context of fiber-integrated devices because conventional fabrication methods of semiconducting nanowires are complex and not adapted to the fiber geometry. [63] Furnace or laser based annealing cannot lead to this type of architectures. Yan et al. reported the simple and robust integration of high-quality monocrystalline Se nanowires into flexible optoelectronic fibers.[157] This innovative approach only consists of three steps: sonication of the exposed amorphous Se in the fiber; soaking the amorphous Se in 1-propanol; and Se nanowires formation from the bulk with their simultaneous interfacing with the surrounding electrodes. The whole process can be accomplished at ambient conditions without any elevated temperatures. In Figure 8d we show the SEM micrographs of the cross-section of the Se core fiber sandwiched by polymer composite electrodes. The nanowire mesh formed after this process is shown, with their contact with one of the electrodes. A high resolution TEM analysis reveals the crystalline nature of the nanowire. By combining electron microscopy as well as first-principle density-functional theory calculations, it was discovered that the solvent played a key role in modulating the interfacial energy of different crystal facets. Selenium in its trigonal phase has a large anisotropy between its basal and prismatic planes. As reveal by calculations, this anisotropy is enhanced by the presence of the solvent. The enhanced anisotropy favored one-dimensional nanowire growth because a crystal plane would grow at a rate proportional to its respective interfacial energy, from the thermodynamic point of view.

Miniaturizing the device by reducing the electrode distance down to the typical length of nanowires enhanced the optoelectronic performance, featuring high photoresponsivity and photosensitivity, low dark currents, low noise-equivalent power, and fast response speeds. Some explanations that may account for the excellent performances include high light trapping efficiency due to the intrinsic properties of the nanowire

mesh, high carrier mobility due to the monocrystalline characteristic and unique crystallographic orientation with respect to the electric field, high-quality interfaces between the nanowires and built-in electrodes, and a limited crystallization depth that is comparable to the photon penetration depth. Most strikingly, this new approach facilitated high throughput and ultra-large area integration of Se nanowires into devices without the need for a complex contacting procedure in the clean room, demonstrated by the growth of high-performance optoelectronic nanowire-based devices along the fiber length. Furthermore, Yan et. al. demonstrated the unique capability of a hybrid fiber for fluorescent imaging based on a single fiber exhibiting simultaneous efficient optical guidance and superior photodetection. Possible further applications of this newly designed fiber structure include remote optical communication systems, detection of weak signals and signals in formerly unreachable areas, minimally invasive in situ and in vivo bio-compatible probing and imaging of biological tissues, as well as large-area, flexible optoelectronics and energy harvesting systems.

6. Discussion

The scientific and technological breakthroughs presented above are allowing the development of fiber-integrated devices at a level of complexity comparable with conventional two-dimensional processing techniques. In this section, we will discuss the latest developments in the field and opportunities for novel applications.

6.1 Novel materials and architectures

Cladding materials

The understanding of the fluid dynamics and rheological properties at play during thermal drawing has opened novel opportunities for polymer materials to play an increasingly important role in the functionality of fiber devices. A major breakthrough lies in the novel rheological criterion exposed in Section 4.4 that gives a simple and fast way to screen materials for attributes compatible with thermal drawing. This is a perfect example of how the deeper fundamental understanding of the processing of thermally-drawn fibers has been essential to allowing novel functionalities and applications. In particular, the different identified thermoplastic elastomers allow a novel way to manufacture stretchable electronic and photonic devices at the scalability and potential cost of optical fibers. Fibers capable of sensing and differentiating a variety of deformations constitute the next generation of sensing networks for soft prosthesis, robotics, and smart textiles. Lowering the elastic modulus of fiber probes for in-vivo applications can also bring novel opportunities in bio-engineering, as discussed below. It will also lead to the discovery of novel materials that could be thermally drawn within complex and functional architectures. Some biodegradable polymers, as well as natural edible polymers, share indeed the same rheological characteristics required for thermal drawing. They could be a basis for the next generation of medical scaffolds, sutures, and other health care applications.

Electrodes

Polymer composites have been exploited both as electrodes, resistors, and as electronic materials with enhanced dielectric properties, as explained in Section 3. The investigation of the fluid dynamics and rheological influence of the fillers on the flow of the polymer matrix in the context of thermal drawing still remains an open field. Indeed, while the technological impact of novel fillers such as carbon nanofibers was demonstrated in the context of neural probes,[112] an analysis at the material and processing levels will bring a deeper insight into the possible fillers and functionalities that could be integrated. One example is the use of one- and two-dimensional fillers such as carbon nanotubes and graphene sheets to bring down the percolation threshold and create transparent and conducting electrodes. This would constitute a major breakthrough for optoelectronic fiber devices as it would allow for sandwich configurations that could be employed to produce more efficient photoconducting and photovoltaic devices. Another research field in need of novel conducting materials is high temperature multi-material fiber systems. As explained above, it is not possible to interface crystalline semiconductors that will melt during the drawing process with crystalline metallic materials. An alternative could be silicate or borosilicate glass nanocomposites that integrate conducting fillers. Just like their polymer counterparts, such composites could exhibit good electrical conductivity while providing viscous domains to contain the flow.

With the introduction of soft polymer cladding, liquid metals have become natural candidates to realize stretchable electronic devices via thermal drawing. These materials possess peculiar properties and are intensively investigated for stretchable electronics devices[158][159][160]. In Figure 9a we show an example of a thermally drawn SEBS fiber integrating two Gallium electrodes[56]. Both the resistance and capacitance between the two wires could change reproducibly with strains, and over tens of thousands of cycles. Combining these materials with the complex architectures shown for example in Figure 7c and 7d is bringing unprecedented sensing capabilities. Having different sensors for a similar signal can enable to compensate for various sources of drift or changes due to temperature, stress relaxation etc… Moreover, several sensors that can discriminate different types of excitations in a single compact platform remains a long-time objective and thermal drawing offers a unique approach to achieve it.

While liquid metals have recently been introduced to the multi-material fiber platform, amorphous solid metals remain unexplored. These materials would constitute an ideal platform in a myriad of applications, especially to create electrodes with high conductivity and small feature size or in configurations where highly conductive and/or reflecting layers are required. Their high viscosity[161,162] during drawing could prevent capillary break-up of small cylinders or thin films. Compositions that can have both a good stability against crystallization and a viscosity comparable with that of thermoplastics, and at similar temperatures, remain to be found.

Dielectric materials

Polymers with high dielectric constants or with piezo- and ferro-electric properties can be exploited in fibers to create large area and flexible ultrasound and vibration sensors, super-capacitor, or fibers that can be

moved or bent. Insulators can also be used as energy harvester via for example Triboelectricity that is widely investigated but has never been achieved within the thermal drawing fiber platform. While the range polymers with the right electrical properties and processing attributes is limited, adding inorganic fillers can enhance the performance and functionality of such systems. An in-depth analysis is required of the trade-off between changing the rheological properties of the polymer matrix as the filler concentration increases, and improving its functional properties. Nanocomposite-based polymers could also constitute interesting matrices for dielectric with tailored optical properties. Novel dielectric materials processed at high temperature within borosilicate or silicate cladding could also bring interesting properties to fiber-based devices but have remained unexplored.

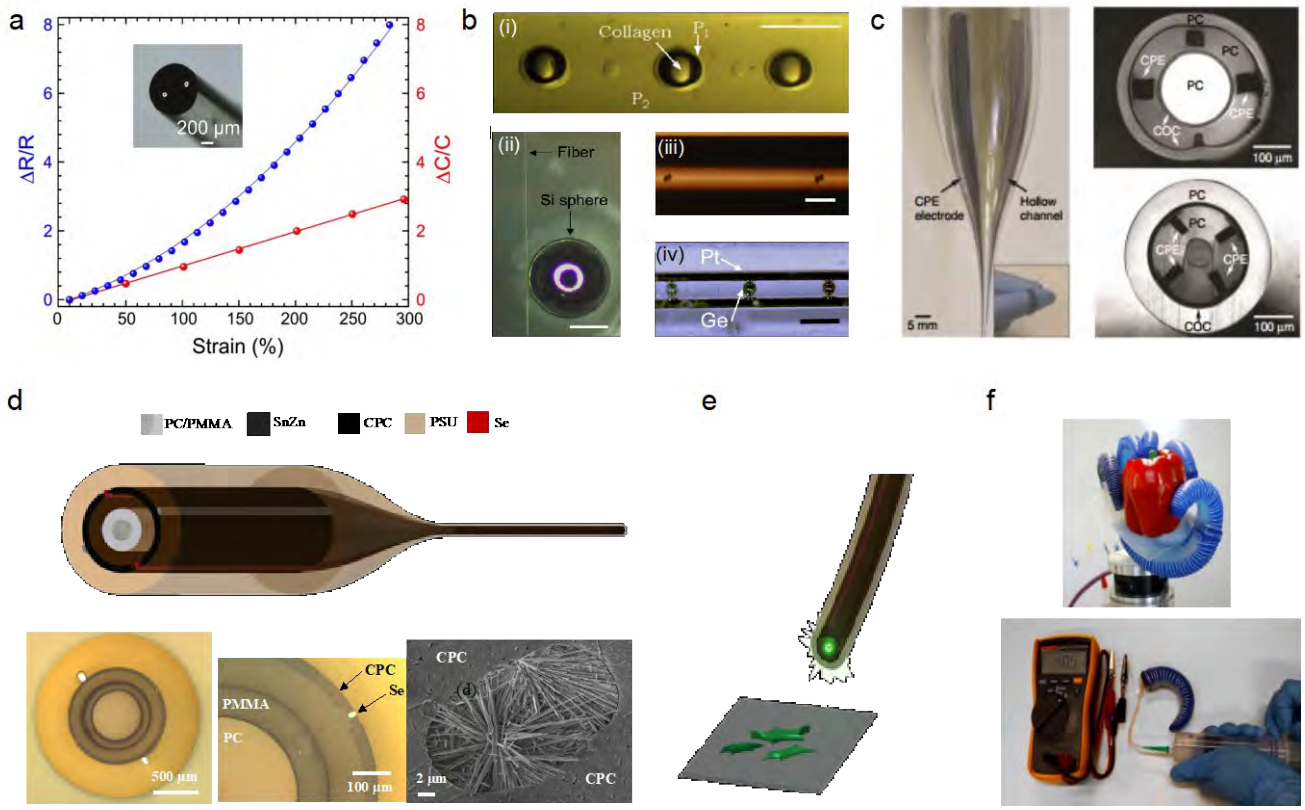

Figure 9

Semiconductors

Having access to a wider range of semiconductor compositions with better microstructures is becoming a significant asset for the integration of complex devices in the fiber form. This aspect is best highlighted by the recently developed ability to grow selenium nanowires in the trigonal phase with few grain boundaries[157]. Selenium is a semiconductor with excellent optoelectronic properties including good free carriers mobility. The particular architecture of the nanowire mesh allows for an excellent absorption of the incoming light, while good extraction of charges is ensured by the nanowire quality. This recent work for the first time achieved optoelectronic performance for fiber integrated devices in terms of sensitivity and response speed on par with conventional two-dimensional devices. This opens truly exciting opportunities to bring fiber-based photodetectors closer to real products. Interesting investigation remains to be done

regarding the influence of nanowire crossing on charge transport. Different strategies to align nanowires as they grow could be explored to minimize scattering at intersections, and to ensure charge transport along a single nanowire. Also, we envision that other anisotropic fiber materials such as Te and Se/Te compounds[163] that can be dissolved in a solvent and subsequently exhibit an exacerbated anisotropy in the interfacial energy can also be compatible with this method for single crystal nanowire growth.

The in-fiber synthesis approach is also an exciting topic for further research, with several opportunities for the integration of high-quality electronic and optoelectronic materials. For example, some excellent chalcogenide-based thermoelectric materials such as SnSe and Bi2Se3 with high melting points [164] might be synthesized in fibers via a similar chemical reaction at a low drawing temperature. Tin sulfide (SnS) is another interesting alloy investigated as a potential candidate for earth abundant photovoltaic materials. [165] Moreover, by designing the preform architecture, the formed semiconductors can interface with metallic electrode or other or semiconducting material, generating heterogeneous junctions. The formation of such junctions could enable fiber-based transistors, light-emitting diodes, lasers, high-speed photodetectors, and solar cells with targeted performance on par with their planar counterparts.. Furthermore, this principle can also be employed to remove detrimental materials in fibers. For example, the addition of SiC to silicon core optical fibers allows the reduction of silica during drawing, resulting in oxygen-free silicon optical fibers. [166] The ability to physically mix disparate materials in fibers and allowing them to chemically react and form novel compounds during drawing increases the complexity and functionalities of fiber devices.

Fiber integrated spheres

Finally, we discuss the implications of multi-material sphere break-up within fibers. The different structures of in-fiber particles realized with by a wide range of functional materials have led to the realization of advanced functions on two levels of control. The first level is the control of a single particle's functionality distribution in the same material. For example, surface functionalization of polymeric particles has been demonstrated for bio-detection through specific protein-protein interactions and volumetric encapsulation of a biomaterial in spherical polymeric shells, as shown in Figure 9b(i). [137] Moreover, an ordered array of silicon-based whispering-gallery mode resonators with a Q factor as high as 7.1×10^5 is achieved, owing to the process-induced ultra-smooth surface and highly crystalline nature, as shown in Figure 9b(ii). [144] The second level is the control of a structured multi-material particle's functionality. For example, the spatially coherent break-up of a dual-core (p-type and n-type silicon) fiber leads to the joining of the particles into a bi-spherical silicon p-n junction, as shown in Figure 9b(iii). [135] A more precise control of the breakup temperature allows for one domain to experience the fluid instability without impacting the other. For example, the semiconducting germanium core is selectively broken up into a series of relatively larger particles, resulting in direct contacts between semiconducting particles and the two continuous platinum filaments to form electrically contacted, self-assembled, and entirely packaged discrete spherical devices distributed within the entire length of the fiber, as shown in Figure 9b(iv). [96]

6.2 Novel applications: integrating multiple functionalities

As we discussed in the introduction and in the first section of this progress report, there are many ways to create functional fibers. One promising method relies on coating textile- or carbon-based fibers to form devices such as piezoelectric sensors, [167] actuators, [168] batteries, [169] or triboelectric energy harvesting[170] devices. Depending on the requirements for a specific application, manufacturing methods are chosen for their efficiency and resulting device performance. However, when several functionalities must be integrated in a single fiber or the targeted applications require the combination of several materials organized in complex nanoscale architectures, methods based on thermal drawing interesting attributes compared to more conventional processes. Here we discuss a few promising applications that require the combination of all of the recent scientific advances discussed in this progress report.

Photodetecting and photovoltaic fibers

Efficient optoelectronic devices require optimization at the material, architecture, and interface levels. Light must be collected as efficiently as possible by the semiconducting materials and the generated charges must be extracted by a built-in or imposed voltage, which requires good bulk and interface properties. Photovoltaic cells in particular require micro- and nanoscale materials for efficient conversion of a diffuse source of energy that is captured over hundreds of square meters. [171,172] In this regard, any innovative and practical approach that can make a significant impact on the energy and PV landscape must entail breakthroughs in materials processing. Thermally drawn fibers constitute an ideal platform to generate extended length of PV fibers that integrate all of the required constituents, which are assembled at the preform level. The advances presented here bring significant breakthroughs in all of the key requirements, including light trapping, charge extraction, and encapsulation. Integrated textures on the surface or within fibers can serve as anti-reflection and light-trapping architectures to better collect light from every incoming direction. The different strategies described to integrate novel semiconducting materials with the proper microstructure, as well as junctions, can generate efficient inorganic light converters. The different types of electrodes discussed can also be chosen to act as efficient contacts along the entire fiber length. The development of single crystal nanowire meshes could also be exploited for highly efficient PV fibers, and research into junction generation and the improvement of contacting solutions is ongoing.

From an engineering point of view, thermal drawing as a packaging solution has also been proposed as an alternative research direction for the integration of optoelectronic functionalities. [173] The idea is to draw already-made planar optoelectronic devices so that the polymer cladding shears the positioned devices that are spaced at roughly equal distances apart along the fiber length. While this approach has limitations in terms of the active surface area that can be functionalized, it can avoid the challenges associated with the compatibility of materials with thermal drawing. Here again, the polymer cladding could be structured to enhance light collection and to ensure proper insulation from the environment.

Fibers for interrogation of neural circuits

Techniques and methodologies capable of dissecting complex neural circuits enable investigation of the function of neural networks and insight into the underlying causes of mental health disorders and neurological diseases. [11,174] Compact and robust systems that can interface with these networks are essential. Highly flexible, miniaturized, and biocompatible multi-material and multi-functional fibers that integrate waveguides, microfluidics channels, and conducting electrode arrays are an ideal platform for these systems. In Figure 9c we show two examples of such fiber architectures integrating polymer composites electrodes, waveguides and microchannels[175]. Such fibers have been shown to allow for simultaneous optical, electrical, and pharmacological interrogation of neural circuits in vivo, [70] and in that case to observe neural activity correlated with optical stimulation and diminished by drug injection. Embedding similar fiber probes in the spinal cord permitted optical control of motor functions by correlating evoked neural activity with behavioral responses. [175] As discussed above, engineering the microstructure of polymer nanocomposites has led to significantly reduced electrode dimension and improved electrical conductivity, which allows for integration of higher density electrodes, optical waveguides, and fluid delivery channels in probes with smaller diameters. [176]. Due to the miniaturization of these fibers, multiple probes could be implanted into different regions of the mouse brain for optogenetic interrogation of neural projection dynamics. Another elegant approach for improving the conductivity of polymer nanocomposites is to introduce biocompatible carbon nanofibers into nanocomposites by virtue of their in situ alignment during the thermal drawing. [112] The resulting neural probe exhibited a miniature footprint and a proper impedance that allowed for stable electrophysiological recording with high fidelity. An alternative to conductive nanocomposites is metallic electrodes. Multiple electrodes with feature sizes as small as 5 μm were integrated into a single fiber probe with a dimension comparable to that of human hair, which enabled a high density of recording sites. [70] We envision that the number of recording electrodes can be drastically increased by the incorporation of novel metallic materials that can overcome capillary instability induced breakup during thermal drawing. Long-term in vivo studies verified that these probes were minimally invasive and featured stable tissue-machine interfaces in the brain. [70][176][112]

Even though the abovementioned probes are flexible, their elastic moduli are not sufficiently low to probe neurons in mammalian spinal cords responsible for organ function and voluntary limb control. Fiber probes that mechanically match the low elastic modulus of neural tissue and tolerate cyclic strain during spinal cord placement were recently demonstrated. [177] The probes consisted of stretchable polymer optical fibers drawn within a thermoplastic cladding. After removal of this cladding, the fiber was coated with conductive silver nanowire meshes to serve as electrodes. In vivo placement in spinal cord tisuse demonstrated that these hybrid probes were capable of acute recording spontaneous neural activity, sensory-evoked potentials, and the simultaneous recording of optically-evoked spinal potentials and optical control of hindlimb muscles. Note that the stretchable component could not be directly drawn and a sacrificial polymer cladding was introduced to encapsulate the soft material during the drawing and was removed afterward. Our recent work

has demonstrated that elastomeric materials with tailored microstructures and proper rheological attributes can be co-processed with conductive elements using a single thermal draw. [56]

Even though current multifunctional fiber probes create important new avenues for basic research into the operation of neural circuits, existing in vivo optogenetic and pharmacological technologies rely on external fibers to deliver light into the tissues and tethered tubing and metal cannula connected to external fluidic infusion pumps. These physical constraints restrict studies on the natural behavior of animals such as social interaction and communication in complex environments. A future direction would be to develop wireless systems in multi-material fibers. For example, near-field wireless communications can supply the power to operate pharmacological fluid delivery systems as well as point-light sources and electrodes for optogenetics. [178]

Electro-mechanical fibers

Recent progress made in regards to electronic materials and achievable architectures has led to fibers that can sense vibration via piezoelectric materials, sense pressure via mechanical bending of flexible domains, and trigger strain via ferroelectric actuation. These systems were obtained within fibers made of thermoplastic claddings that remain stiff and are not appropriate for applications where deformations must be either measured or induced. The recently developed ability to thermally draw elastomeric materials in the same conditions as thermoplastics has opened a wide range of novel opportunities. Systems used to measure deformation still face difficulties in localizing mechanical excitation over long lengths or large surface areas, and it remains challenging to distinguish between strain, pressure, shear, or twist. The unique ability of thermally-drawn fibers to integrate complex architectures and allow for different functionalities constitutes an interesting approach to the realization of large-scale and smart deformation sensors. Single fibers could integrate architectures to sense and localize pressure, while others could respond to strain or twist independently. In Figure 9f we show an example of application where a stretchable fiber is used to measure the deformation of a robotic “Pneuflex” finger[56,179]. The diverse functionalities that can be integrated in a single fiber could be used to sense deformation but also the pressure and shear applied at the fiber tip, as discussed in the same work.

The integration of multiple architectures and functionalities required in these applications raise another question in regards to the density of devices that can be integrated within fibers. Advanced functionalities can also result from the collective response of many devices working in concert. The Moore’s law for fibers, a concept first introduced by Prof. Fink (Massachusetts Institute of Technology) is another exciting topic of research. Increasing the density of devices in a single fiber requires that the feature size of devices can be scaled down as small as possible while maintaining their functionalities. The discovery and design of new materials that meet this requirement during thermal drawing is needed. Another approach to create density is to assemble several fibers together into meshes and fabrics. In a last paragraph we discuss briefly the challenges and opportunities associated with the use of multimaterial fibers to functionalize different textiles.

6.3 Fiber assembly and advanced textiles

We will end this progress report by discussing a field of application for advanced fibers – in smart textiles – that expose several engineering challenges that must be overcome in order to employ electronic and optoelectronic fibers in real-world applications. The creation of textiles with advanced functionalities has become one of the key scientific and technological challenges in advanced manufacturing today. Smart textiles are envisioned as becoming a major platform in health and personalized care, sports, or robotics. Policy makers and funding agencies see, within the realm of advanced manufacturing, functional fibers and textiles as an important scientific and technological platform to develop and invest in. The traditional textile industries but also the medTech, health care and pharmaceutical, and the entertainment sector are giving an increasing interest to fiber-based solutions. An excellent example of this interest is the recent creation of the Advanced Fibers and Fabrics of America (AFFOA) institute by Prof. Fink at MIT, which is part of the National Network of Manufacturing Innovation (NNMI) Institutes. Consequent funding both from government and industrial partners was raised to create the next generation of functional and connected textiles. As we discussed in introduction, there are several strategies that have been developed to functionalize textile fibers, or to deposit materials directly onto textiles. The difficulties that remain to address from an engineering and product point of view are however still significant. Functional textiles must sustain several washing and drying cycles, and must remain operational even if handled with little care.

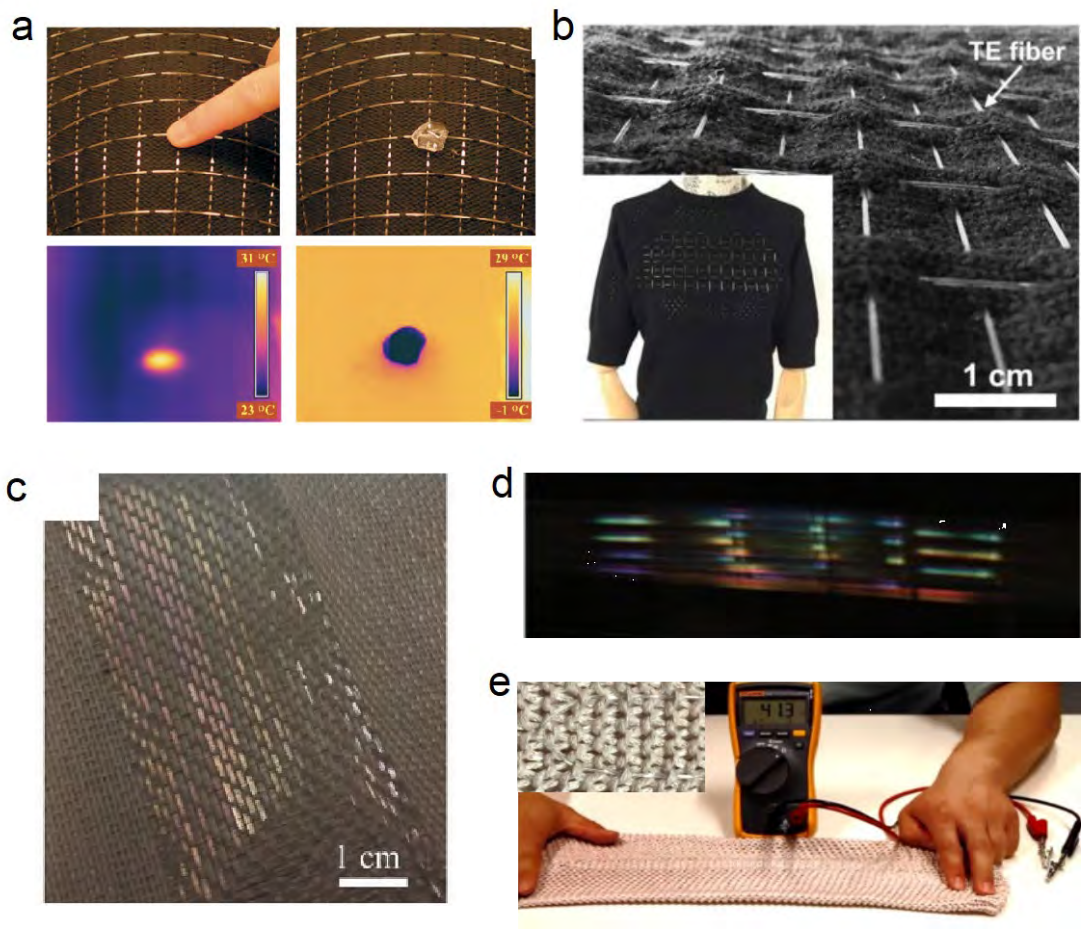

Figure 10: a. A thermal sensing fiber integrated in a fabric that can sense heat from a finger and cold ice[107].

Connecting electrically or optically the integrated functional fibers is a challenge, energy storage and battery lifetime remains a concern, and the integration of the fibers in the textile must be simple and efficient to ensure minimum production cost.

Thermally drawn fibers possess some interesting assets to address these challenges. Their mechanical properties especially at smaller diameters make them amenable to the integration within textile using a variety of techniques such as knitting and weaving at industrial scale. The ability to thermally draw elastomers is a strong asset in that regards[56]. The functional materials are integrated within a cladding that can protect them against the different harsh external conditions that can be found in washing machines and dryers, as well as in everyday life. Thermally drawn fibers can also be imparted with complex functionalities that can bring high added value to a textile product. A single fiber grid was demonstrated to be able to image rudimentary object via a phase retrieval algorithm, quite an advanced optical task[87]. In Figure 10a and b, we show textile integrated thermally drawn fibers that can act as heat sensors[107] or thermoelectric[108] devices, respectively. The ability to design fibers with complex cross-sectional architectures that can be exploited to break the axial symmetry and retrieve information along the fiber length can also have interesting advantages. A particular example is the detection of pressure points that was demonstrated to be possible with only two end connections, with a precision of sub-millimeter along extended fiber length[56,76]. This is particularly attractive for functional textile such as pressure sensing textile, since such a fiber can be weaved across the whole textile while requiring limited connectivity at one fiber end.

In addition to the integration of material architectures within fibers, some functionalities can be imparted via the fiber shape and surface texture as discussed at different places in this manuscript. This favorably compares to fibers that acquire functionalities by coating materials that can be subject to deterioration especially during washing, or non-uniform function. In particular, tailoring hydrophobicity or optical effects can be done thanks to textures at the micrometer and sub-micrometer length scales. As we explained in Section 4.1, arbitrary textures can be fabricated uniformly along the axial and azimuthal direction of various polymer fibers. In Figure10c and 10d, a textile[127] and an assembly of fibers[126] having diffraction gratings and exhibiting color effects can be seen, respectively. that exemplify this novel opportunities enable by the understanding of thermal reflow during drawing.

Finally, as we discuss in the previous sub-section, stretchable fibers is opening exciting opportunities particularly for deformation sensing. Soft fibers are also good candidates for knitting and weaving owing to their peculiar mechanical attributes. In Figure 10e we show such a fiber that has a SEBS cladding that encapsulates a liquid metal electrode. Such fiber, that has sustained standard washing tests, can act as a robust strain sensor to monitor the deformation of fabrics in a variety of contexts such as robotics or soft prosthetics[56]. From all these different examples enabled by the recent breakthroughs described in Sections 3 to 5, it is clear that advanced textiles is a great driving force for the field multi-material fibers in terms of industrial interest and applications.

Conclusion

The filed of multi-material fibers is experiencing a thriving momentum. Policy makers and funding agencies have highlighted functional fibers and textiles as a key advanced manufacturing challenge to be tackled. Industrial funding and interest is raising and the number of academic groups investing in fiber drawing capabilities and joining this field is on a steep raise. This paradigm is the result of the recent turn in the field to tackle the materials science and engineering bottlenecks and develop a deeper scientific onto which to develop a strong foundation for the field. It insures that the opportunities and limitations are well evaluated, and steer applied research towards the right applications. Indeed, this evolution has come in pair with novel engineering solutions and application opportunities that has strengthened support from industry. In this progress report, we critically analyzed recent results in terms of their scientific novelty and the opportunities they offer for future research and applications. Settling on these two pillars is crucial for the multi-material fiber field to continue to develop itself and propose impactful outcome for science and society. We hope that our report reveals the depth of this research field which is at the crossroad of materials science and processing, fluid mechanics, rheology, optics, physics of semiconductors, and electronics. It is also a research topic that is rich of fundamental questions to be addressed, out of which direct industrial ventures are possible. We also hope that will trigger the interest of more researchers in related and orthogonal fields, but also of science and engineering students who would like to engage in an applied field full of interesting materials science and engineering questions to address.

Acknowledgement

The authors would like to acknowledge the Swiss National Science Foundation (Grant No. 200021_146871), and the European Research Council (ERC Starting Grant 679211 “FLOWTONICS”) for their funding support. This work was supported in part by the Singapore Ministry of Education Academic Research Fund Tier 2 (MOE2015-T2-1-066 and MOE2015-T2-2-010), Singapore Ministry of Education Academic Research Fund Tier 1 (RG85/16), and Nanyang Technological University (Start-up grant M4081515: Lei Wei).

References

[1] J. a Rogers, T. Someya, Y. Huang, *Science (80-.).* **2010**, *327*, 1603.

[2] L. Xu, S. R. Gutbrod, A. P. Bonifas, Y. Su, M. S. Sulkin, N. Lu, H. J. Chung, K. I. Jang, Z. Liu, M. Ying, C. Lu, R. C. Webb, J. S. Kim, J. I. Laughner, H. Cheng, Y. Liu, A. Ameen, J. W. Jeong, G. T. Kim, Y. Huang, I. R. Efimov, J. a. Rogers, *Nat. Commun.* **2014**, *5*, 1.

[3] Y. Xia, J. a. Rogers, K. E. Paul, G. M. Whitesides, *Chem. Rev.* **1999**, *99*, 1823.

[4] M. L. Hammock, A. Chortos, B. C. K. Tee, J. B. H. Tok, Z. Bao, *Adv. Mater.* **2013**, *25*, 5997.

[5] A. F. Abouraddy, M. Bayindir, G. Benoit, S. D. Hart, K. Kuriki, N. Orf, O. Shapira, F. Sorin, B. Temelkuran, Y. Fink, **2007**, *6*.

[6] W. Zeng, L. Shu, Q. Li, S. Chen, F. Wang, X. M. Tao, *Adv. Mater.* **2014**, *26*, 5310.

[7] W. Weng, P. Chen, S. He, X. Sun, H. Peng, *Angew. Chemie - Int. Ed.* **2016**, *55*, 6140.

[8] J. S. Heo, J. Eom, Y.-H. Kim, S. K. Park, *Small* **2017**, *1703034*, 1703034.

[9] L. Zhang, S. Lin, T. Hua, B. Huang, S. Liu, X. Tao, *Adv. Energy Mater.* **2018**, *8*, 1.

[10] G. Y. Chen, D. G. Lancaster, T. M. Monro, *Sensors* **2017**, *18*, 72.

[11] R. Chen, A. Canales, P. Anikeeva, *Nat. Rev. Mater.* **2017**, *2*, 16093.

[12] H. Zhu, W. Luo, P. N. Ciesielski, Z. Fang, J. Y. Zhu, G. Henriksson, M. E. Himmel, L. Hu, *Chem. Rev.* **2016**, *116*, 9305.

[13] P. Polygerinos, Z. Wang, K. C. Galloway, R. J. Wood, C. J. Walsh, *Rob. Auton. Syst.* **2015**, *73*, 135.

[14] B. Weintraub, Y. Wei, Z. L. Wang, B. Weintraub, Y. Wei, Z. L. Wang, *Angew. Chemie - Int. Ed.* **2009**, *48*, 8981.

[15] Z. L. Wang, J. Chen, L. Lin, *Energy Environ. Sci.* **2015**, *8*, 2250.

[16] M. Stoppa, A. Chiolerio, *Sensors (Switzerland)* **2014**, *14*, 11957.

[17] Y. Qin, X. Wang, Z. L. Wang, *Nature* **2008**, *451*, 809.

[18] Z. Yang, H. Sun, T. Chen, L. Qiu, Y. Luo, H. Peng, *Angew. Chemie - Int. Ed.* **2013**, *52*, 7545.

[19] T. Chen, L. Qiu, H. G. Kia, Z. Yang, H. Peng, *Adv. Mater.* **2012**, *24*, 4623.

[20] X. Pu, L. Li, M. Liu, C. Jiang, C. Du, Z. Zhao, W. Hu, Z. L. Wang, *Adv. Mater.* **2016**, *28*, 98.

[21] X. He, Y. Zi, H. Guo, H. Zheng, Y. Xi, C. Wu, J. Wang, W. Zhang, C. Lu, Z. L. Wang, *Adv. Funct. Mater.* **2017**, *27*, 1.

[22] M. R. Lee, R. D. Eckert, K. Forberich, G. Dennler, C. J. Brabec, R. a Gaudiana, *Science* **2009**, *324*, 232.

[23] T. L. Andrew, L. Zhang, N. Cheng, M. Baima, J. J. Kim, L. Allison, S. Hoxie, *Acc. Chem. Res.* **2018**, acs. accounts.7b00604.

[24] Z. Wen, M. H. Yeh, H. Guo, J. Wang, Y. Zi, W. Xu, J. Deng, L. Zhu, X. Wang, C. Hu, L. Zhu, X. Sun, Z. L. Wang, *Sci. Adv.* **2016**, *2*, DOI 10.1126/sciadv.1600097.

[25] H. Jinno, K. Fukuda, X. Xu, S. Park, Y. Suzuki, M. Koizumi, T. Yokota, I. Osaka, K. Takimiya, T. Someya, *Nat. Energy* **2017**, *2*, 780.

[26] L. Lao, L. Fu, G. Qi, E. P. Giannelis, J. Fan, *ACS Appl. Mater. Interfaces* **2017**, *9*, 38109.

[27] Y. Guo, X.-S. Zhang, Y. Wang, W. Gong, Q. Zhang, H. Wang, J. Brugger, *Nano Energy* **2018**, *48*, 152.

[28] N. Matsuhisa, M. Kaltenbrunner, T. Yokota, H. Jinno, K. Kuribara, T. Sekitani, T. Someya, *Nat. Commun.* **2015**, *6*, 1.

[29] N. Karim, S. Afroj, S. Tan, P. He, A. Fernando, C. Carr, K. S. Novoselov, *ACS Nano* **2017**, *11*, 12266.

[30] J. Zhong, Y. Zhang, Q. Zhong, Q. Hu, B. Hu, Z. L. Wang, J. Zhou, *ACS Nano* **2014**, *8*, 6273.

[31] H. Sun, Y. Zhang, J. Zhang, X. Sun, H. Peng, *Nat. Rev. Mater.* **2017**, *2*, 1.

[32] T. Huang, C. Wang, H. Yu, H. Wang, Q. Zhang, M. Zhu, *Nano Energy* **2014**, *14*, 226.

[33] M. Tebyetekerwa, Z. Xu, W. Li, X. Wang, I. Marriam, S. Peng, S. Ramkrishna, S. Yang, M. Zhu, *ACS Appl. Energy Mater.* **2017**, acsaem.7b00057.

[34] X. Z. Yao Lu, Chen Chen, *Functional Nanofibers for Energy Storage*, **n.d.**

[35] S. Chen, W. Ma, H. Xiang, Y. Cheng, S. Yang, W. Weng, M. Zhu, *J. Power Sources* **2016**, *319*, 271.

[36] B. M. Quandt, L. J. Scherer, L. F. Boesel, M. Wolf, G. L. Bona, R. M. Rossi, *Adv. Healthc. Mater.* **2015**, *4*, 330.

[37] A. Lund, K. Rundqvist, E. Nilsson, L. Yu, B. Hagström, C. Müller, *npj Flex. Electron.* **2018**, *2*, 9.

[38] B. Temelkuran, S. D. Hart, G. Benoit, J. D. Joannopoulos, Y. Fink, *Nature* **2002**, *420*, 650.

[39] M. Bayindir, F. Sorin, A. F. Abouraddy, J. Viens, S. D. Hart, J. D. Joannopoulos, Y. Fink, *Nature* **2004**, *431*, 826.

[40] S. Egusa, Z. Wang, N. Chocat, Z. M. Ruff, A. M. Stolyarov, D. Shemuly, F. Sorin, P. T. Rakich, J. D. Joannopoulos, Y. Fink, *Nat. Mater.* **2010**, *9*, 643.

[41] A. F. Abouraddy, O. Shapira, M. Bayindir, J. Arnold, F. Sorin, D. S. Hinczewski, J. D. Joannopoulos, Y. Fink, *Nat. Mater.* **2006**, *5*, 532.

[42] M. Bayindir, O. Shapira, D. Saygin-Hinczewski, J. Viens, A. F. Abouraddy, J. D. Joannopoulos, Y. Fink, *Nat. Mater.* **2005**, *4*, 820.

[43] G. Tao, A. M. Stolyarov, A. F. Abouraddy, *Int. J. Appl. Glas. Sci.* **2012**, *3*, 349.

[44] M. Alexander Schmidt, A. Argyros, F. Sorin, *Adv. Opt. Mater.* **2016**, *4*, 13.

[45] G. Tao, A. F. Abouraddy, A. M. Stolyarov, **2015**, *56*, 1.

[46] J. D. Joannopoulos, Y. Fink, **2004**, *3*, 2004.

[47] S. D. Hart, G. R. Maskaly, B. Temelkuran, P. H. Prideaux, J. D. Joannopoulos, Y. Fink, *Science* **2002**, *296*, 510.

[48] M. Yaman, T. Khudiyev, E. Ozgur, M. Kanik, O. Aktas, E. O. Ozgur, H. Deniz, E. Korkut, M. Bayindir, *Nat. Mater.* **2011**, *10*, 494.

[49] J. J. Kaufman, G. Tao, S. Shabahang, D. S. Deng, Y. Fink, A. F. Abouraddy, *Nano Lett.* **2011**, *11*, 4768.

[50] G. Tao, S. Shabahang, E.-H. Banaei, J. J. Kaufman, A. F. Abouraddy, *Opt. Lett.* **2012**, *37*, 2751.

[51] M. Zhu, X. Wang, Z. Pan, C. Cheng, Q. Zhu, C. Jiang, Q. Nie, P. Zhang, Y. Wu, S. Dai, T. Xu, G. Tao, X. Zhang, *Appl. Phys. A Mater. Sci. Process.* **2015**, *119*, 455.

[52] G. Tao, S. Shabahang, H. Ren, Z. Yang, X. Wang, A. F. Abouraddy, **2014**, *8982*, 898223.

[53] R. Mossadegh, J. S. Sanghera, D. Schaafsma, B. J. Cole, V. Q. Nguyen, R. E. Miklos, I. D. Aggarwal, *J. Light. Technol.* **1998**, *16*, 214.

[54] S. S. Habahang, F. a T. An, J. D. P. Erlstein, G. T. Ao, a Lvarez, F. C. Henard, a S. Incore, L. S. Hah, R. Ichardson, K. L. S. Chepler, a F. a Bouraddy, **2017**, *7*, 2336.

[55] K. Cook, G. Balle, J. Canning, L. Chartier, T. Athanaze, M. a. Hossain, C. Han, J.-E. Comatti, Y. Luo, G.-D. Peng, *Opt. Lett.* **2016**, *41*, 4554.

[56] Y. Qu, **n.d.**

[57] H. W. Lee, M. a. Schmidt, R. F. Russell, N. Y. Joly, H. K. Tyagi, P. Uebel, P. S. J. Russell, *Opt. Express* **2011**, *19*, 12180.

[58] P. Uebel, M. a. Schmidt, M. Scharrer, P. S. J. Russell, *New J. Phys.* **2011**, *13*, DOI 10.1088/1367-2630/13/6/063016.

[59] P. S. Westbrook, B. J. Eggleton, R. S. Windeler, A. Hale, T. a. Strasser, G. L. Burdge, *IEEE Photonics Technol. Lett.* **2000**, *12*, 495.

[60] N. Da, L. Wondraczek, M. a. Schmidt, N. Granzow, P. S. J. Russell, *J. Non. Cryst. Solids* **2010**, *356*, 1829.

[61] R. Kornbluh, Q. Pei, J. Joseph, V. Bharti, X. Zhao, T. Zama, W. Takashima, K. Kaneto, K. Oguro, Y. Nishimura, M. Mizuhata, H. Takenaka, N. Gebhart, K. J. Kim, M. Shahinpoor, J. P. Gong, Y. Osada, H. Okuzaki, H. Hori, D. C. Lagoudas, H. Y. Jun, R. D. Allen, C. Cui, J. Su, Z. Iqbal, a a Zakhidov, a C. Arsenault, I. Manners, G. a Ozin, W. F. Paxton, T. E. Mallouk, a Sen, S. Subramanian, a Schwartz, N. Bowden, G. M. Whitesides, *Science (80-.).* **2006**, *311*, 1583.

[62] J. R. Sparks, P. J. Sazio, V. Gopalan, J. V Badding, *Templated Chemically Deposited Semiconductor Optical Fiber Materials*, **2013**.

[63] G. Kostovski, P. R. Stoddart, A. Mitchell, *Adv. Mater.* **2014**, *26*, 3798.

[64] N. M. Y. Zhang, K. Li, T. Zhang, P. Shum, Z. Wang, Z. Wang, N. Zhang, J. Zhang, T. Wu, L. Wei, *ACS Photonics* **2018**, *5*, 347.

[65] N. Yu, F. Capasso, *J. Light. Technol.* **2015**, *33*, 2344.

[66] E. J. Smythe, M. D. Dickey, G. M. Whitesides, F. Capasso, *October* **2009**, *3*, 59.

[67] D. J. Lipomi, R. V. Martinez, M. a. Kats, S. H. Kang, P. Kim, J. Aizenberg, F. Capasso, G. M. Whitesides, *Nano Lett.* **2011**, *11*, 632.

[68] M. Consales, M. Pisco, A. Cusano, *Photonic Sensors* **2012**, *2*, 289.

[69] X. D. Wang, O. S. Wolfbeis, *Anal. Chem.* **2013**, *85*, 487.

[70] A. Canales, X. Jia, U. P. Froriep, R. a Koppes, C. M. Tringides, J. Selvidge, C. Lu, C. Hou, L. Wei, Y. Fink, P. Anikeeva, *Nat. Biotechnol.* **2015**, *2*, 1.

[71] A. M. Stolyarov, L. Wei, F. Sorin, G. Lestoquoy, J. D. Joannopoulos, Y. Fink, *Appl. Phys. Lett.* **2012**, *101*, 11108.

[72] A. M. Stolyarov, L. Wei, O. Shapira, F. Sorin, S. L. Chua, J. D. Joannopoulos, Y. Fink, *Nat. Photonics* **2012**, *6*, 229.

[73] N. Zhang, H. Liu, A. M. Stolyarov, T. Zhang, K. Li, P. P. Shum, Y. Fink, X. W. Sun, L. Wei, *ACS Photonics* **2016**, *3*, 2275.

[74] H. Knape, W. Margulis, *Opt. Lett.* **2007**, *32*, 614.

[75] F. Sorin, G. Lestoquoy, S. Danto, J. D. Joannopoulos, Y. Fink, *Opt. Express* **2010**, *18*, 24264.

[76] T. Nguyen-Dang, A. G. Page, Y. Qu, M. Volpi, W. Yan, F. Sorin, *J. Phys. D. Appl. Phys.* **2017**, *50*, DOI 10.1088/1361-6463/aa5bf7.

[77] S. Gorgutsa, J. F. Gu, M. Skorobogatiy, *Smart Mater. Struct.* **2011**, *21*, 15010.

[78] X. Lu, H. Qu, M. Skorobogatiy, *Sci. Rep.* **2017**, *7*, 1.

[79] G. Lestoquoy, N. Chocat, Z. Wang, J. D. Joannopoulos, Y. Fink, *Appl. Phys. Lett.* **2013**, *102*, DOI 10.1063/1.4802783.

[80] N. Chocat, G. Lestoquoy, Z. Wang, D. M. Rodgers, J. D. Joannopoulos, Y. Fink, *Adv. Mater.* **2012**, *24*, 5327.

[81] S. Wang, T. Zhang, K. Li, S. Ma, M. Chen, P. Lu, L. Wei, *Adv. Electron. Mater.* **2017**, *3*, 1.

[82] S. Danto, F. Sorin, N. D. Orf, Z. Wang, S. A. Speakman, J. D. Joannopoulos, Y. Fink, *Adv. Mater.* **2010**, *22*, 4162.

[83] M. Bayindir, a. F. Abouraddy, J. Arnold, J. D. Joannopoulos, Y. Fink, *Adv. Mater.* **2006**, *18*, 845.

[84] S. Danto, Z. Ruff, Z. Wang, J. D. Joannopoulos, Y. Fink, *Adv. Funct. Mater.* **2011**, *21*, 1095.

[85] X. Z. J-L Adam, *Chalcogenide Glasses Preparation, Properties and Applications*, **n.d.**

[86] J. Rowlands, S. Kasap, *Phys. Today* **1997**, *50*, 24.

[87] F. Sorin, O. Shapira, A. F. Abouraddy, M. Spencer, N. D. Orf, J. D. Joannopoulos, Y. Fink, *Nano Lett.* **2009**, *9*, 2630.

[88] A. Gumennik, A. M. Stolyarov, B. R. Schell, C. Hou, G. Lestoquoy, F. Sorin, W. McDaniel, A. Rose, J. D. Joannopoulos, Y. Fink, *Adv. Mater.* **2012**, *24*, 6005.

[89] G. Tang, Q. Qian, X. Wen, G. Zhou, X. Chen, M. Sun, D. Chen, Z. Yang, *J. Alloys Compd.* **2015**, *633*, 1.

[90] G. Tang, Q. Qian, X. Wen, X. Chen, W. Liu, M. Sun, Z. Yang, *Opt. Express* **2015**, *23*, 23624.

[91] S. H. P. Eng, G. U. T. Ang, K. A. H. Uang, Q. I. Q. Ian, D. O. C. Hen, Q. I. Z. Hang, Z. H. Y. Ang, **2017**, *7*, 1647.

[92] C. Hou, X. Jia, L. Wei, A. M. Stolyarov, O. Shapira, J. D. Joannopoulos, Y. Fink, *Nano Lett.* **2013**, *13*, 975.

[93] N. D. Orf, O. Shapira, F. Sorin, S. Danto, M. a. Baldo, J. D. Joannopoulos, Y. Fink, *Proc. Natl. Acad. Sci.* **2011**, *108*, 4743.

[94] J. Ballato, T. Hawkins, P. Foy, B. Yazgan-Kokuoz, C. McMillen, L. Burka, S. Morris, R. Stolen, R. Rice, *Opt. Fiber Technol.* **2010**, *16*, 399.

[95] a. C. Peacock, U. J. Gibson, J. Ballato, *Adv. Phys. X* **2016**, *1*, 114.

[96] L. Wei, C. Hou, E. Levy, G. Lestoquoy, A. Gumennik, A. F. Abouraddy, J. D. Joannopoulos, Y. Fink, *Adv. Mater.* **2016**, 1.

[97] M. Rein, E. Levy, A. Gumennik, A. F. Abouraddy, J. Joannopoulos, Y. Fink, *Nat. Commun.* **2016**, *7*, 1.

[98] R. He, P. J. a. Sazio, A. C. Peacock, N. Healy, J. R. Sparks, M. Krishnamurthi, V. Gopalan, J. V. Badding, *Nat. Photonics* **2012**, *6*, 174.

[99] R. He, T. D. Day, M. Krishnamurthi, J. R. Sparks, P. J. a Sazio, V. Gopalan, J. V. Badding, *Adv. Mater.* **2013**, *25*, 1461.

[100] F. a. Martinsen, B. K. Smeltzer, M. Nord, T. Hawkins, J. Ballato, U. J. Gibson, *Sci. Rep.* **2014**, *4*, 1.

[101] J. R. Sparks, R. He, N. Healy, M. Krishnamurthi, A. C. Peacock, P. J. A. Sazio, V. Gopalan, J. V. Badding, *Adv. Mater.* **2011**, *23*, 1647.

[102] a C. Peacock, N. Healy, *Semicond. Sci. Technol.* **2016**, *31*, DOI Artn 10300410.1088/0268-1242/31/10/103004.

[103] A. C. Peacock, J. R. Sparks, N. Healy, *Laser Photonics Rev.* **2014**, *8*, 53.

[104] N. Healy, U. Gibson, A. C. Peacock, **2018**.

[105] J. Ballato, T. Hawkins, P. Foy, C. McMillen, L. Burka, J. Reppert, R. Podila, a M. Rao, R. R. Rice, *Opt. Express* **2010**, *18*, 4972.

[106] D. a. Coucheron, M. Fokine, N. Patil, D. W. Breiby, O. T. Buset, N. Healy, A. C. Peacock, T. Hawkins, M. Jones, J. Ballato, U. J. Gibson, *Nat. Commun.* **2016**, *7*, 13265.

[107] M. Bayindir, A. F. Abouraddy, J. Arnold, J. D. Joannopoulos, Y. Fink, *Adv. Mater.* **2006**, *18*, 845.

[108] T. Zhang, K. Li, J. Zhang, M. Chen, Z. Wang, S. Ma, N. Zhang, L. Wei, *Nano Energy* **2017**, *41*, 35.

[109] T. Zhang, K. Li, C. Li, S. Ma, H. H. Hng, L. Wei, **2017**, *3*, 1.

[110] T. Khudiyev, J. Clayton, E. Levy, N. Chocat, A. Gumennik, A. M. Stolyarov, J. Joannopoulos, Y. Fink, *Nature* **n.d.**, *8*, 1.

[111] X. Lu, H. Qu, M. Skorobogatiy, *ACS Nano* **2017**, *11*, 2103.

[112] Y. Guo, S. Jiang, B. J. B. Grena, I. F. Kimbrough, E. G. Thompson, Y. Fink, H. Sontheimer, T. Yoshinobu, X. Jia, *ACS Nano* **2017**, *11*, 6574.

[113] T.-C. Lin, J. Zhao, C. Cao, A. Javadi, Y. Yang, I. Hwang, X. Li, *J. Micro Nano-Manufacturing* **2016**, *4*, 41008.

[114] C. Hou, X. Jia, L. Wei, S.-C. Tan, X. Zhao, J. D. Joannopoulos, Y. Fink, *Nat. Commun.* **2015**, *6*, 6248.

[115] D. Li, A. Babel, S. a. Jenekhe, Y. Xia, *Adv. Mater.* **2004**, *16*, 2062.

[116] H. Chen, J. Di, N. Wang, H. Dong, J. Wu, Y. Zhao, J. Yu, L. Jiang, *Small* **2011**, *7*, 1779.

[117] J. T. McCann, M. Marquez, Y. Xia, *J. Am. Chem. Soc.* **2006**, *128*, 1436.

[118] J. Wu, N. Wang, Y. Zhao, L. Jiang, *J. Mater. Chem. A* **2013**, *1*, 7290.

[119] J. Fu, S. Das, G. Xing, T. Ben, V. Valtchev, S. Qiu, *J. Am. Chem. Soc.* **2016**, *138*, 7673.

[120] S. S. J. Hollister, *Nat. Mater.* **2005**, *4*, 518.

[121] B. Grena, J. B. Alayrac, E. Levy, A. M. Stolyarov, J. D. Joannopoulos, Y. Fink, *Nat. Commun.* **2017**, *8*, DOI 10.1038/s41467-017-00375-0.

[122] B. Grena, Phase Separation in Thermally-Drawn Fibers: From Porous Domains to Structured Si-Ge Spheres, **2017**.

[123] R. A. Koppes, S. Park, T. Hood, X. Jia, N. Abdolrahim Poorheravi, A. H. Achyuta, Y. Fink, P. Anikeeva, *Biomaterials* **2016**, *81*, 27.

[124] A. F. A. Esmaeil-Hooman Banaei, *Prog. Photovoltaics Res. Appl.* **2013**, *23*, 403.

[125] A. Yildirim, M. Yunusa, F. E. Ozturk, M. Kanik, M. Bayindir, *Adv. Funct. Mater.* **2014**, *24*, 4569.

[126] T. Nguyen-Dang, A. C. de Luca, W. Yan, Y. Qu, A. G. Page, M. Volpi, T. Das Gupta, S. P. Lacour, F.

Sorin, *Adv. Funct. Mater.* **2017**, 1605935.

[127] T. Khudiyev, C. Hou, A. M. Stolyarov, Y. Fink, *Adv. Mater.* **2017**, 1605868.

[128] D. S. Deng, J. C. Nave, X. Liang, S. G. Johnson, Y. Fink, *Opt. Express* **2011**, *19*, 16273.

[129] D. S. Deng, N. D. Orf, A. F. Abouraddy, A. M. Stolyarov, J. D. Joannopoulos, H. A. Stone, Y. Fink, *Nano Lett.* **2008**, *8*, 4265.

[130] T. Khudiyev, O. Tobail, M. Bayindir, *Sci. Rep.* **2014**, *4*, 4864.

[131] J. Zhao, A. Javadi, L. T. Chiang, I. Hwang, Y. Yang, Z. Guan, X. Li, *J. Micro Nano-Manufacturing* **2016**, *4*, 1.

[132] S. Xue, G. W. Barton, S. Fleming, A. Argyros, *J. Light. Technol.* **2017**, *35*, 2167.

[133] O. T. Naman, M. R. New-Tolley, R. Lwin, A. Tuniz, a. H. Al-Janabi, I. Karatchevtseva, S. C. Fleming, B. T. Kuhlmey, A. Argyros, *Adv. Opt. Mater.* **2013**, *1*, 971.

[134] J. Zhao, X. Li, *J. Micro Nano-Manufacturing* **2017**, *6*, 11003.

[135] A. Gumennik, L. Wei, G. Lestoquoy, A. M. Stolyarov, X. Jia, P. H. Rekemeyer, M. J. Smith, X. Liang, B. J.-B. Grena, S. G. Johnson, S. Gradečak, A. F. Abouraddy, J. D. Joannopoulos, Y. Fink, *Nat. Commun.* **2013**, *4*, 2216.

[136] J. J. Kaufman, G. Tao, S. Shabahang, E.-H. Banaei, D. S. Deng, X. Liang, S. G. Johnson, Y. Fink, A. F. Abouraddy, *Nature* **2012**, *487*, 463.

[137] J. J. Kaufman, R. Ottman, G. Tao, S. Shabahang, E.-H. Banaei, X. Liang, S. G. Johnson, Y. Fink, R. Chakrabarti, A. F. Abouraddy, *Proc. Natl. Acad. Sci.* **2013**, *110*, 15549.

[138] O. Aktas, E. Ozgur, O. Tobail, M. Kanik, E. Huseyinoglu, M. Bayindir, *Adv. Opt. Mater.* **2014**, *2*, 618.

[139] T. Khudiyev, O. Tobail, M. Bayindir, *Sci. Rep.* **2014**, *4*, 4864.

[140] G. Tao, J. J. Kaufman, S. Shabahang, R. Rezvani Naraghi, S. V. Sukhov, J. D. Joannopoulos, Y. Fink, A. Dogariu, A. F. Abouraddy, *Proc. Natl. Acad. Sci.* **2016**, *113*, 201601777.

[141] A. Alchalaby, R. Lwin, A. H. Al-Janabi, P. W. Trimby, S. C. Fleming, B. T. Kuhlmey, A. Argyros, *J. Light. Technol.* **2016**, *34*, 2198.

[142] M. Vermillac, J. F. Lupi, F. Peters, M. Cabié, P. Vennéguès, C. Kucera, T. Neisius, J. Ballato, W. Blanc, *J. Am. Ceram. Soc.* **2017**, *100*, 1814.

[143] A. Gumennik, E. C. Levy, B. Grena, C. Hou, M. Rein, A. F. Abouraddy, J. D. Joannopoulos, Y. Fink, *Proc. Natl. Acad. Sci.* **2017**, *114*, 7240.

[144] J. Zhang, K. Li, T. Zhang, P. J. S. Buenconsejo, M. Chen, Z. Wang, M. Zhang, Z. Wang, L. Wei, *Adv. Funct. Mater.* **2017**, *27*, 1.

[145] M. Fokine, A. Theodosiou, S. Song, T. Hawkins, J. Ballato, K. Kalli, U. J. Gibson, *Opt. Mater. Express* **2017**, *7*, 1589.

[146] W. Yan, T. D. Nguyen, C. Cayron, T. Dasgupta, A. G. Page, Y. Qu, F. Sorin, **2017**, *7*, 1135.

[147] N. Gupta, C. McMillen, R. Singh, R. Podila, a. M. Rao, T. Hawkins, P. Foy, S. Morris, R. Rice, K. F. Poole, L. Zhu, J. Ballato, *J. Appl. Phys.* **2011**, *110*, DOI 10.1063/1.3660270.

[148] S. Morris, C. McMillen, T. Hawkins, P. Foy, R. Stolen, J. Ballato, R. Rice, *J. Cryst. Growth* **2012**, *352*, 53.

[149] C. McMillen, G. Brambilla, S. Morris, T. Hawkins, P. Foy, N. Broderick, E. Koukharenko, R. Rice, J. Ballato, *Opt. Mater. (Amst).* **2010**, *32*, 862.

[150] S. Shaudhuri, J. R. Sparks, X. Ji, M. Krishnamurthi, L. Shen, N. Healy, A. C. Peacock, V. Gopalan, J. V. Badding, *ACS Photonics* **2016**, *3*, 378.

[151] D. S. Deng, N. D. Orf, S. Danto, a. F. Abouraddy, J. D. Joannopoulos, Y. Fink, *Appl. Phys. Lett.* **2010**, *96*, 23102.

[152] Y. F. Ranz, A. F. J. R. Unge, H. R. En, N. H. Ealy, K. I. Gnatyev, M. J. Ones, T. H. Awkins, J. B. Allato, U. J. G. Ibson, A. C. P. Eacock, **2017**, *7*, 2055.

[153] J. Dauchot, a Watillon, *J. Colloid Interface Sci.* **1967**, *23*, 62.

[154] N. Healy, M. Fokine, Y. Franz, T. Hawkins, M. Jones, J. Ballato, A. C. Peacock, U. J. Gibson, *Adv. Opt. Mater.* **2016**, 1004.

[155] X. Ji, S. Lei, S.-Y. Yu, H. Y. Cheng, W. Liu, N. Poilvert, Y. Xiong, I. Dabo, S. E. Mohney, J. V. Badding, V. Gopalan, *ACS Photonics* **2016**, acsphotonics.6b00584.

[156] N. Healy, S. Mailis, N. M. Bulgakova, P. J. a Sazio, T. D. Day, J. R. Sparks, H. Y. Cheng, J. V Badding, A. C. Peacock, *Nat. Mater.* **2014**, *13*, 1.

[157] W. Yan, Y. Qu, T. Das Gupta, A. Darga, D. T. Nguyên, A. G. Page, M. Rossi, M. Ceriotti, F. Sorin, *Adv. Mater.* **2017**, *1700681*, 1700681.

[158] M. D. Dickey, *Adv. Mater.* **2017**, *29*, 1.

[159] S. Zhu, J. H. So, R. Mays, S. Desai, W. R. Barnes, B. Pourdeyhimi, M. D. Dickey, *Adv. Funct. Mater.* **2013**, *23*, 2308.

[160] C. B. Cooper, K. Arutselvan, Y. Liu, D. Armstrong, Y. Lin, M. R. Khan, J. Genzer, M. D. Dickey, *Adv. Funct. Mater.* **2017**, *27*, DOI 10.1002/adfm.201605630.

[161] Y. Liu, Y. Zhu, F. Li, W. Yan, *Adv. Eng. Mater.* **2010**, *12*, 1131.

[162] W. Yan, Y. Liu, Y. Zhu, S. Niu, **n.d.**, 435.

[163] Y. Xia, P. Yang, Y. Sun, Y. Wu, B. Mayers, B. Gates, Y. Yin, F. Kim, H. Yan, *Adv. Mater.* **2003**, *15*, 353.

[164] L.-D. Zhao, S.-H. Lo, Y. Zhang, H. Sun, G. Tan, C. Uher, C. Wolverton, V. P. Dravid, M. G. Kanatzidis, *Nature* **2014**, *508*, 373.

[165] R. E. Banai, M. W. Horn, J. R. S. Brownson, *Sol. Energy Mater. Sol. Cells* **2016**, *150*, 112.

[166] S. Morris, T. Hawkins, P. Foy, C. McMillen, J. Fan, L. Zhu, R. Stolen, R. Rice, J. Ballato, *Opt. Mater. Express* **2011**, *1*, 1141.

[167] L. Persano, C. Dagdeviren, Y. Su, Y. Zhang, S. Girardo, D. Pisignano, Y. Huang, J. a. Rogers, *Nat. Commun.* **2013**, *4*, 1610.

[168] Z. F. Liu, S. Fang, F. a. Moura, J. N. Ding, N. Jiang, J. Di, M. Zhang, X. Lepró, D. S. Galvão, C. S. Haines, N. Y. Yuan, S. G. Yin, D. W. Lee, R. Wang, H. Y. Wang, W. Lv, C. Dong, R. C. Zhang, M. J.

Chen, Q. Yin, Y. T. Chong, R. Zhang, X. Wang, M. D. Lima, R. Ovalle-Robles, D. Qian, H. Lu, R. H. Baughman, *Science (80-.).* **2015**, *349*, 400.

[169] D. Yu, Q. Qian, L. Wei, W. Jiang, K. Goh, J. Wei, J. Zhang, Y. Chen, *Chem. Soc. Rev.* **2015**, *44*, 647.

[170] J. Wang, X. Li, Y. Zi, S. Wang, Z. Li, L. Zheng, F. Yi, S. Li, Z. L. Wang, *Adv. Mater.* **2015**, *27*, 4830.

[171] W. Zhou, Z. Wen, P. Gao, *Adv. Energy Mater.* **2018**, *1702512*, 1702512.

[172] B. Brudieu, a. Le Bris, J. Teisseire, F. Guillemot, G. Dantelle, S. Misra, P. R. I. Cabarrocas, F. Sorin, T. Gacoin, *Adv. Opt. Mater.* **2014**, *2*, 1105.

[173] M. R. Yoel Fink, *Thermally-Drawn Fiber Including Devices*, **n.d.**

[174] S. P. Lacour, G. Courtine, J. Guck, *Nat. Rev. Mater.* **2016**, *1*, 16063.

[175] C. Lu, U. P. Froriep, R. a. Koppes, A. Canales, V. Caggiano, J. Selvidge, E. Bizzi, P. Anikeeva, *Adv. Funct. Mater.* **2014**, *24*, 6594.

[176] S. Park, Y. Guo, X. Jia, H. K. Choe, B. Grena, J. Kang, J. Park, C. Lu, A. Canales, R. Chen, Y. S. Yim, G. B. Choi, Y. Fink, P. Anikeeva, *Nat. Neurosci.* **2017**, *20*, 612.

[177] C. Lu, S. Park, T. J. Richner, A. Derry, I. Brown, C. Hou, S. Rao, J. Kang, C. T. Mortiz, Y. Fink, P. Anikeeva, *Sci. Adv.* **2017**, *3*, e1600955.

[178] G. Shin, A. M. Gomez, R. Al-Hasani, Y. R. Jeong, J. Kim, Z. Xie, A. Banks, S. M. Lee, S. Y. Han, C. J. Yoo, J. L. Lee, S. H. Lee, J. Kurniawan, J. Tureb, Z. Guo, J. Yoon, S. Il Park, S. Y. Bang, Y. Nam, M. C. Walicki, V. K. Samineni, A. D. Mickle, K. Lee, S. Y. Heo, J. G. McCall, T. Pan, L. Wang, X. Feng, T. Il Kim, J. K. Kim, Y. Li, Y. Huang, R. W. Gereau, J. S. Ha, M. R. Bruchas, J. a. Rogers, *Neuron* **2017**, *93*, 509.

[179] R. Deimel, O. Brock, *Int. J. Rob. Res.* **2016**, *35*, 161.